Supplementary Information

Pd-oxazolone complexes conjugated to an engineered enzyme: Improving fluorescence and catalytic properties

Carla Garcia-Sanz[†a], Alicia Andreu[†a], Blanca de las Rivas[b], Ana I. Jiménez[c], Alexandra Pop[d], Cristian Silvestru[d], Esteban P. Urriolabeitia*[c] and Jose M. Palomo*[a]

[a] Department of Biocatalysis, Institute of Catalysis (ICP-CSIC), Marie Curie 2, 28049 Madrid, Spain.

E-mail: josempalomo@icp.csic.es

[b] Department of Microbial Biotechnology, Institute of Food Science, Technology and Nutrition (ICTAN-CSIC), José Antonio Novais 10, 28040 Madrid, Spain

[c] Instituto de Síntesis Quimica y Catálisis Homogénea (ISQCH, CSIC-Universidad de Zaragoza), C/Pedro Cerbuna 12, Zaragoza, E-50009, Spain

Email: esteban@unizar.es

[d] Supramolecular Organic and Organometallic Chemistry Centre, Department of Chemistry, Faculty of Chemistry and Chemical Engineering, Babeş-Bolyai University, Str. Arany Janos 11, RO-400028 Cluj−Napoca, Romania

Table S1: Crystal data for 5a

Empirical formula	$C_{23}H_{21}NO_6Pd$
Formula Weight	513.81
Temperature	100(2) K
Wavelength	0.71073 Å
Crystal system, space group	monoclinic, $P2_1/c$
Unit cell dimensions	a = 11.0443(12) Å b = 23.315(3) Å β = 92.790(1)° c = 7.9061(9) Å
Volume	2033.4(4) Å³
Z	4
Absorption coefficient	0.954 mm^{-1}
F(000)	1040
Crystal Size	0.065 x 0.160 x 0.240 mm
Absorption correction	Multi-scan
T_{min} , T_{max}	0.7420, 0.9010
θ_{min},θ_{max}	1.747, 28.300
Limiting indices	$-14\leq h\leq 14$, $-31\leq k\leq 27$, $-10\leq l\leq 10$
Reflections collected / unique	20669 / 5043 [R(int) = 0.0500]
Completeness to θ_{max}	99.6% (100 % up to θ =25.24°)
Refinement method	Full-matrix least-squares on F^2
Data / restraints / parameters	5043 / 0 / 319
Goodness-of-fit on F^2	1.025
Final R indices [I>2sigma(I)]	R1=0.0302; wR2=0.0619 [3808 refl.]
R indices (all data)	R1=0.0549; wR2=0.0695
Largest diff. peak and hole	0.511 / -0.691

Table S2. Selected bond lengths (Å) and angles (°) for 5a

Pd(1)-O(5)	2.0184(18)	O(5)-Pd(1)-N(1)	175.51(8)
Pd(1)-O(6)	2.0869(18)	O(5)-Pd(1)-C(1)	87.14(9)
Pd(1)-N(1)	2.044(2)	O(6)-Pd(1)-N(1)	91.46(8)
Pd(1)-C(1)	1.984(2)	O(6)-Pd(1)-C(1)	175.02(9)
O(5)-Pd(1)-O(6)	90.36(7)	N(1)-Pd(1)-C(1)	90.73(10)

Table S3. Fluorescence studies of complexes **4a**, **4b**, **and 5** in pure acetonitrile.

Sample	Pd content (ppm)	Excitation λ (nm)	Emission λ (nm)	Intensity (counts)
4a	100	450	525	16.29
4a	250	450	537	0.95
4a	100	475	525	28.64
4a	250	475	533	1.54
4b	100	450	560	24.50
4b	250	450	575	1.61
4b	100	475	561	11.58
4b	250	475	580	1.32
5a	100	450	527	48.69
5a	250	450	534	22.20
5a	100	475	527	62.32
5a	250	475	534	23.61

Table S4. Fluorescence studies of complexes **4a**, **4b**, **and 5** in 20% acetonitrile: 80% water pH 7.

Sample	Pd content (ppm)	Excitation λ (nm)	Emission λ (nm)	Intensity (counts)
4a	100	450	526.88	22.83
4a	250	450	531.88	13.72
4a	100	475	526.88	26.34
4a	250	475	531.88	16.49
4b	100	450	553.99	3.07
4b	250	450	579.86	1.40
4b	100	475	553.99	7.02
4b	250	475	579.86	2.03
5a	100	450	534.27	8.21
5a	250	450	560.97	5.33
5a	100	475	534.27	9.95
5a	250	475	560.97	7.01

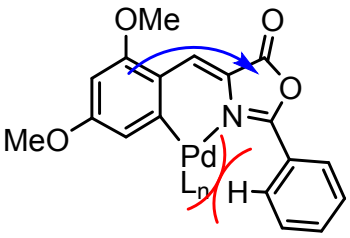

Orthopalladated (**1a**)
Intramolecular repulsions
Push-pull effect

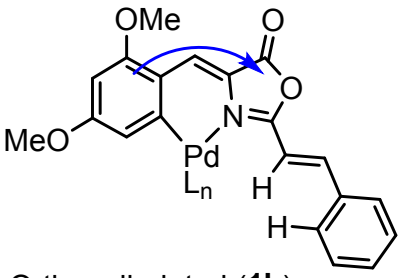

Orthopalladated (**1b**)
Less intramolecular repulsions
Push-pull effect

Figure S1

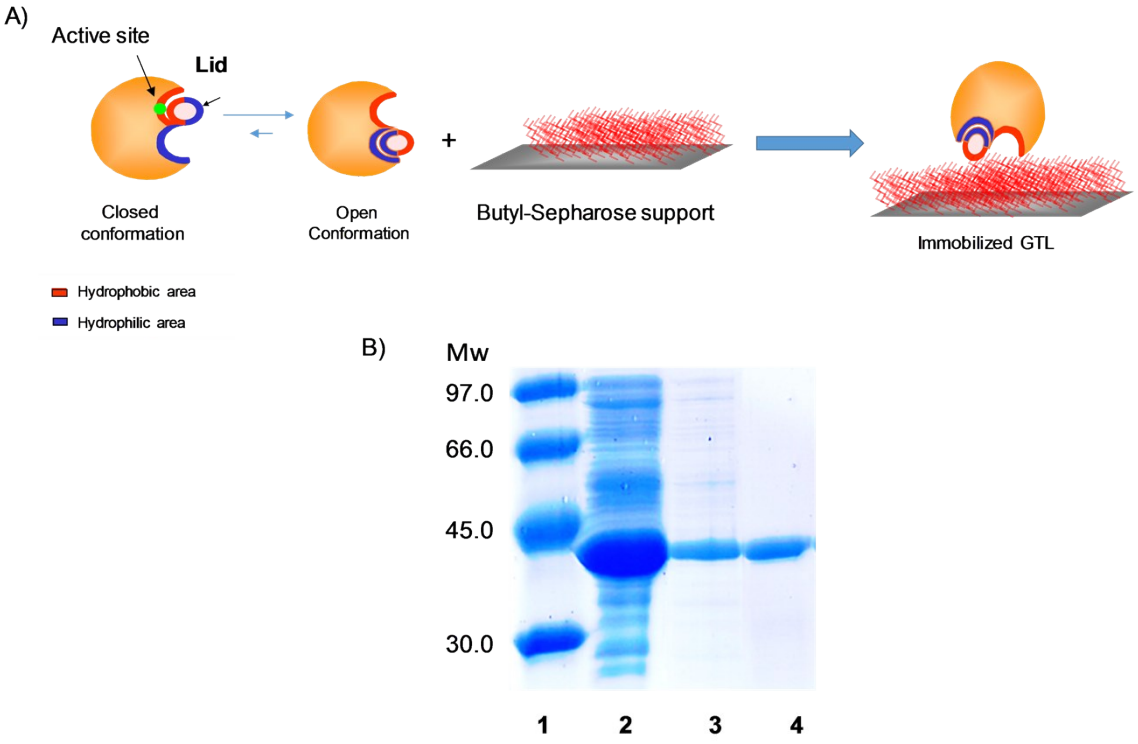

Figure S2. Solid-phase adsorption of GTL variants. A) Strategy of the selective immobilization. B) SDS-PAGE. Lane 1: low-weight molecular marker; Lane 2: GTL or GTL-C114 extract from *E. coli*; Lane 3: GTL absorbed on Butyl-Sepharose; Lane 4: GTL-C114 adsorbed on Butyl-Sepharose.

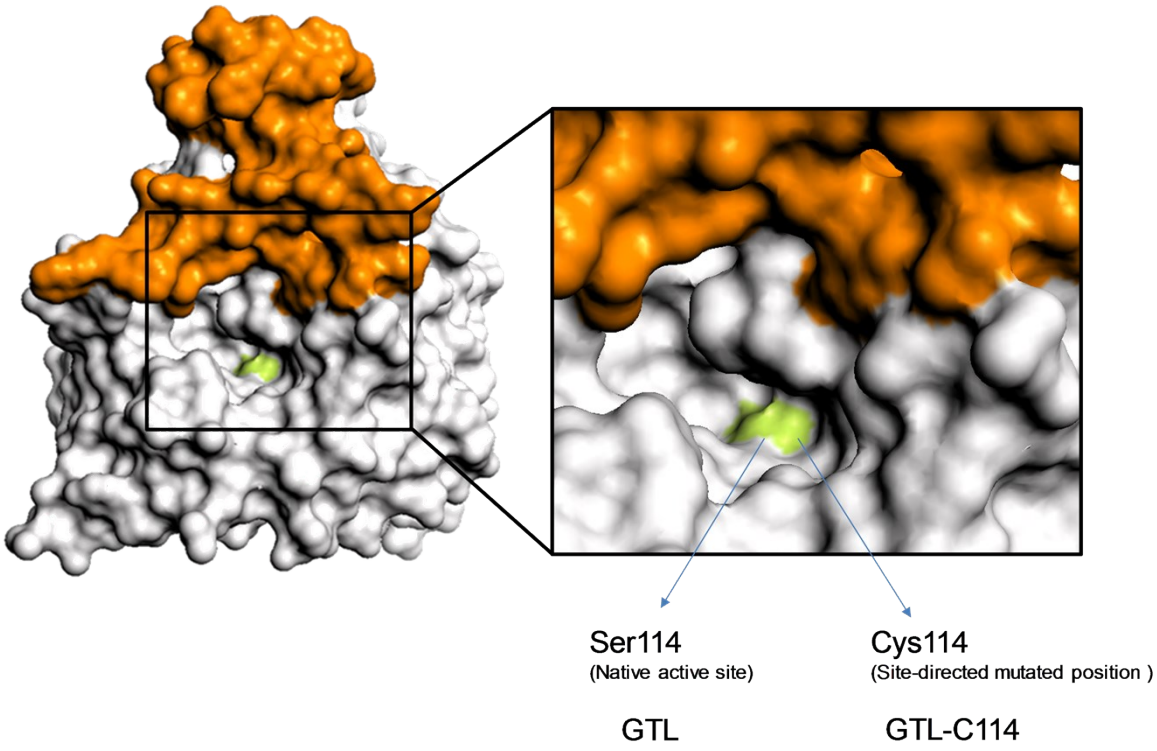

Figure S3. Surface representation of the structure *of G. thermocatenulatus* lipase variants in open conformation. The protein structure was obtained from the Protein Data Bank (pdb code: 2W22) and the picture was created using Pymol v. 0.99.

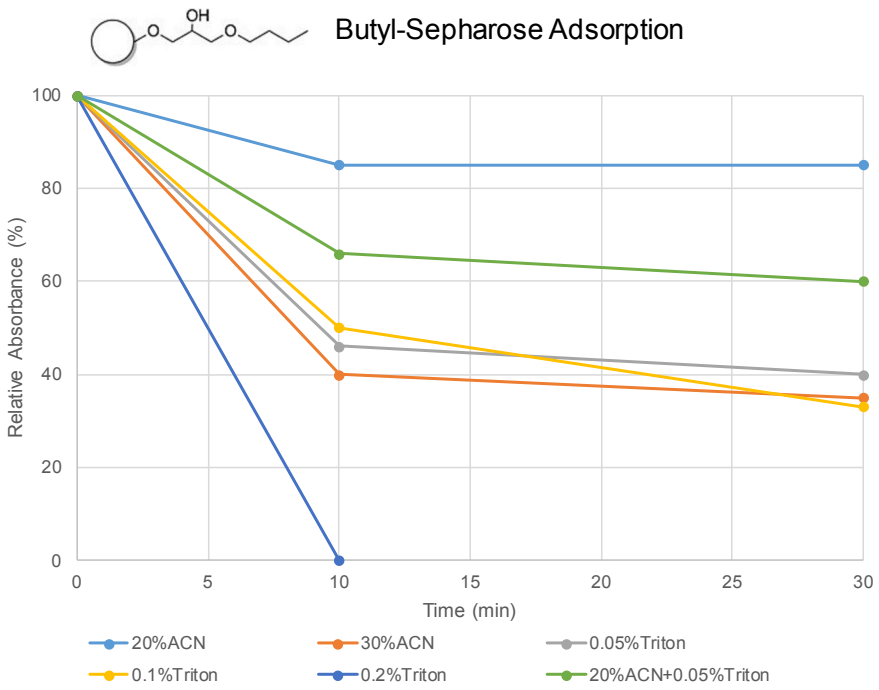

Figure S4. Absorbance of Pd-complex **4a** supernatant after incubation with butyl-Sepharose in aqueous media. Adsorption conditions: 200 µl of 10 mg/ml solution of **4a** in acetonitrile were added to: 180 µl ACN + 1.620 mL water pH 7 (20%ACN); 360 µl ACN + 1.4 mL water pH 7 (30%ACN); 1.8 mL Triton solution (0.05%, 0.1% or 0.2% Triton X-100 solution); 180 µl ACN + 1.620 mL Triton solution (0.05%) (20%ACN+0.05%Triton).

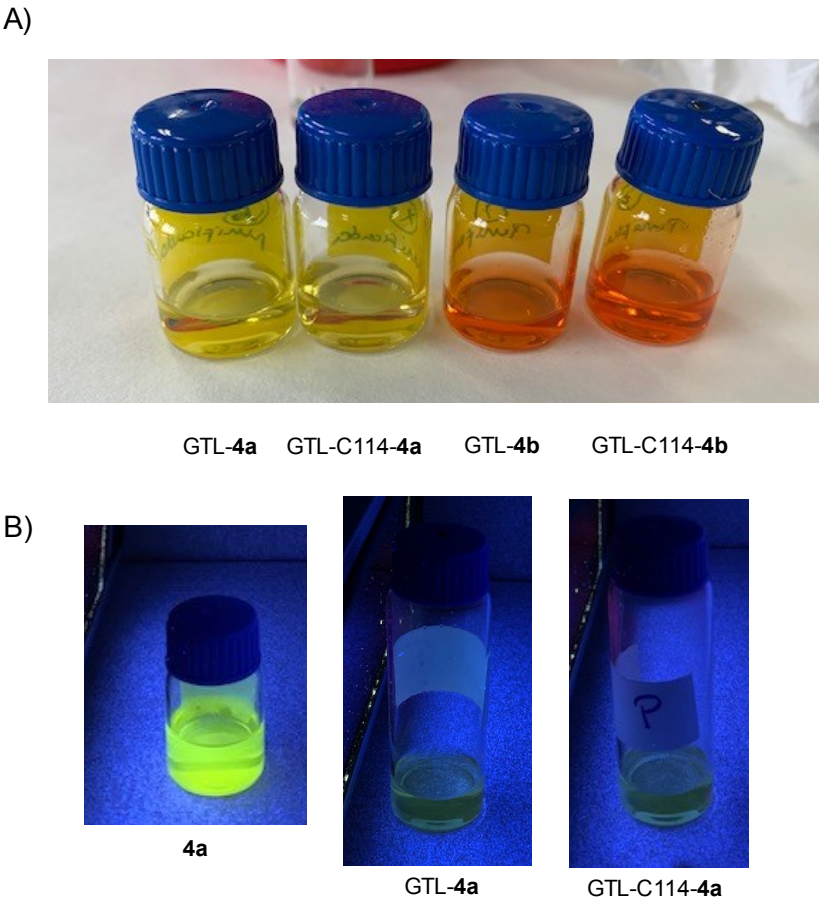

Figure S5. Samples of the novel GTL enzyme-Pd complexes conjugates. A) visible colour samples of the pure conjugates in solution. B) Samples under 365nm-UV light of free **4a** (500 ppm) and conjugates (0.31 ppm) in aqueous solution with 20% acetonitrile.

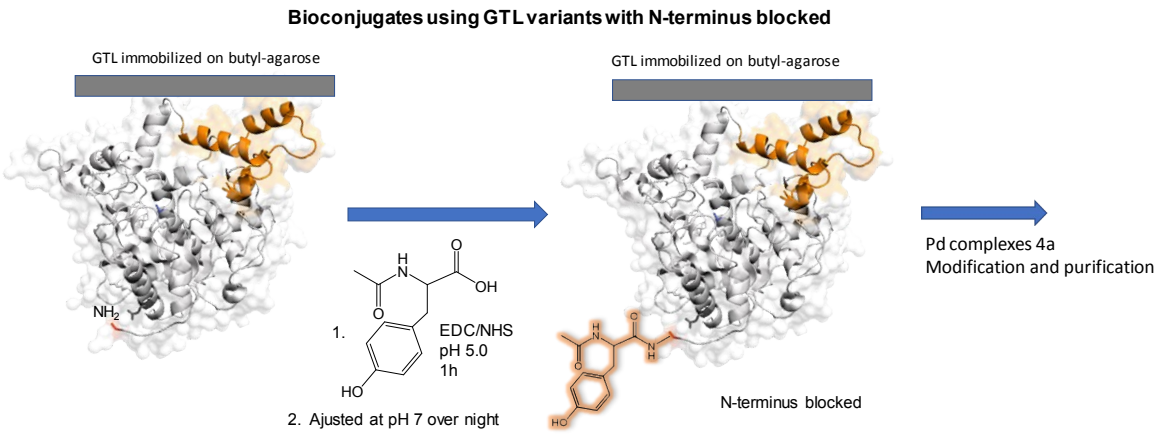

Figure S6. Scheme of the chemical modification of N-terminus of GTL by Ac-Tyr.

A) GTL N-terminal
blocked conjugated with **4a**

B) GTL-114 N-terminal/SH-active site
blocked conjugated with **4a**

Figure S7. Photo of the final purified bioconjugate solution. A. GTL-**4a.** B. GTL114-**4a**.

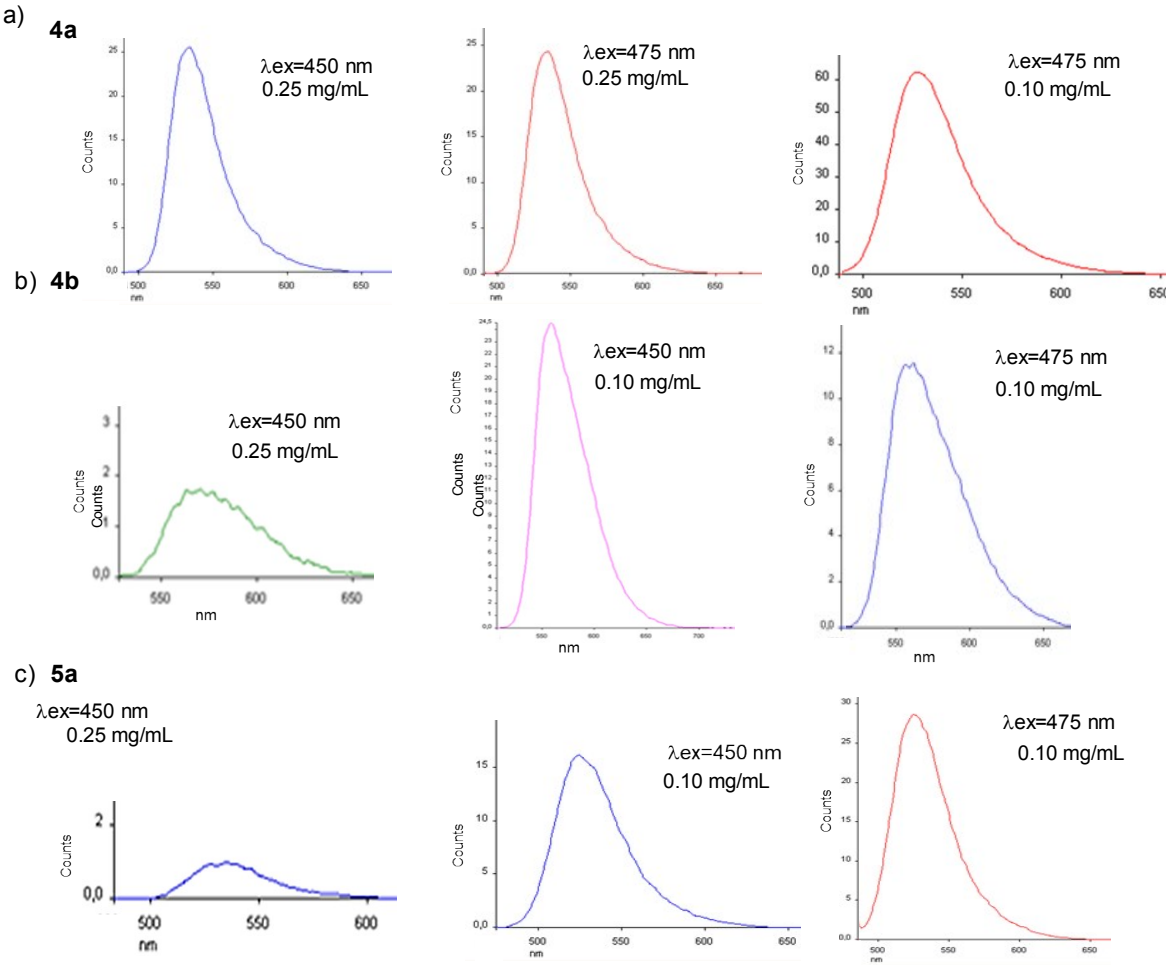

Figure S8. Fluorescence emission spectra of **4a**,**4b** and **5a** in pure acetonitrile. The values of maximum emission have been included in Table 2.

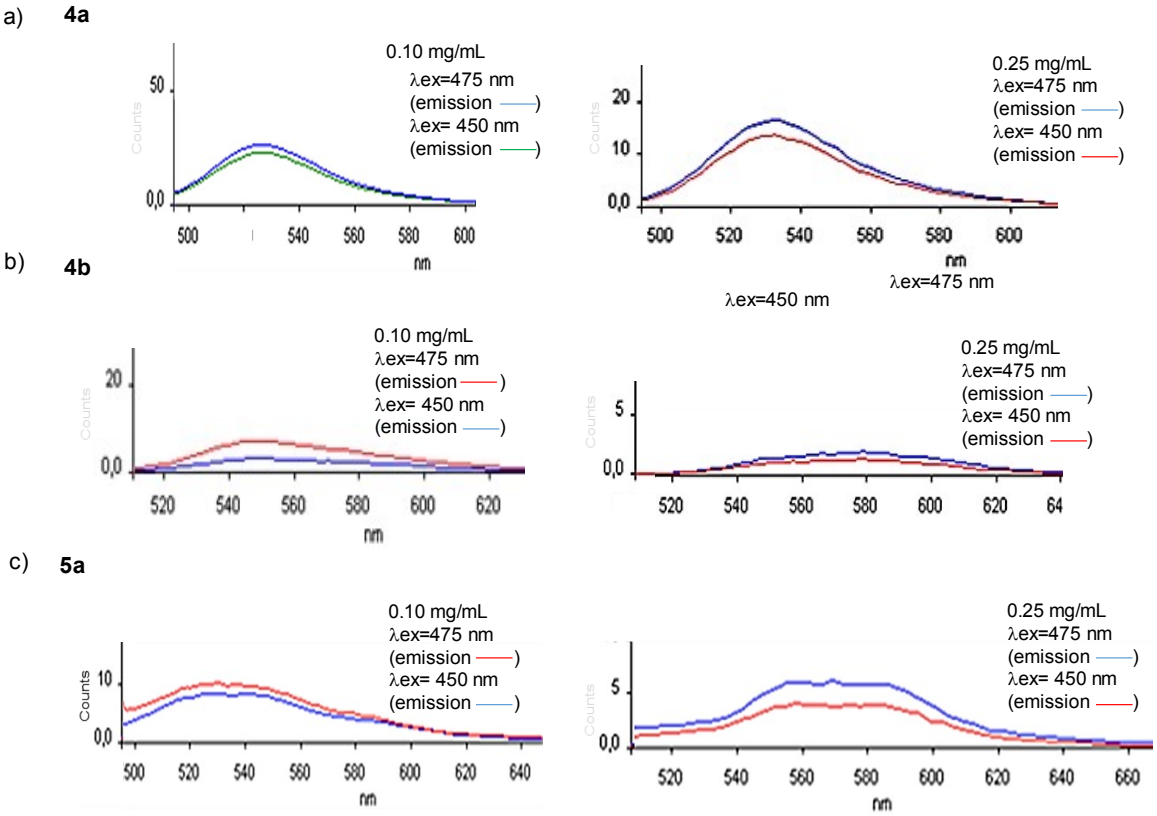

Figure S9. Fluorescence emission spectra of **4a**,**4b** and **5a** in 20% acetonitrile: 80% water pH 7. The values of maximum emission have been included in Table 2.

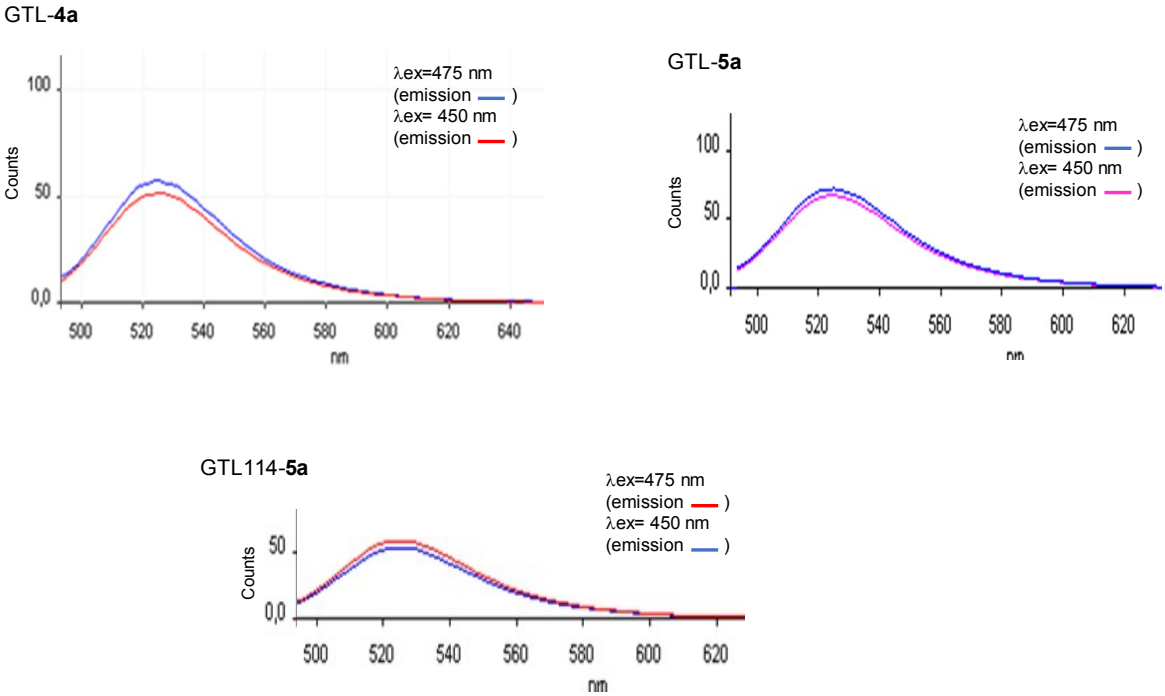

Figure S10. Fluorescence emission spectra of the different synthesized bioconjugates at excitation wavelength of 450 or 475 nm. The values of maximum emission have been included in Table 2.

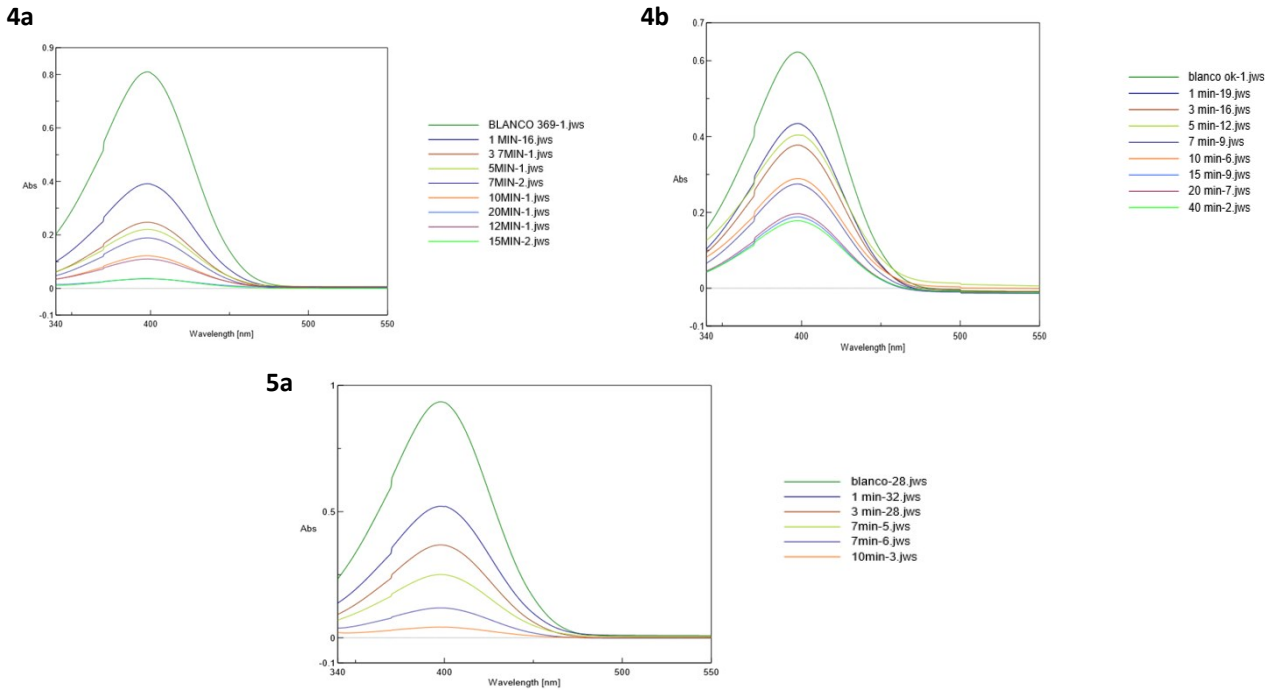

Figure S11. Time-dependent absorption spectra of the Pd-catalyzed reduction of pNP in the presence of different Pd oxazolones and $NaBH_4$.

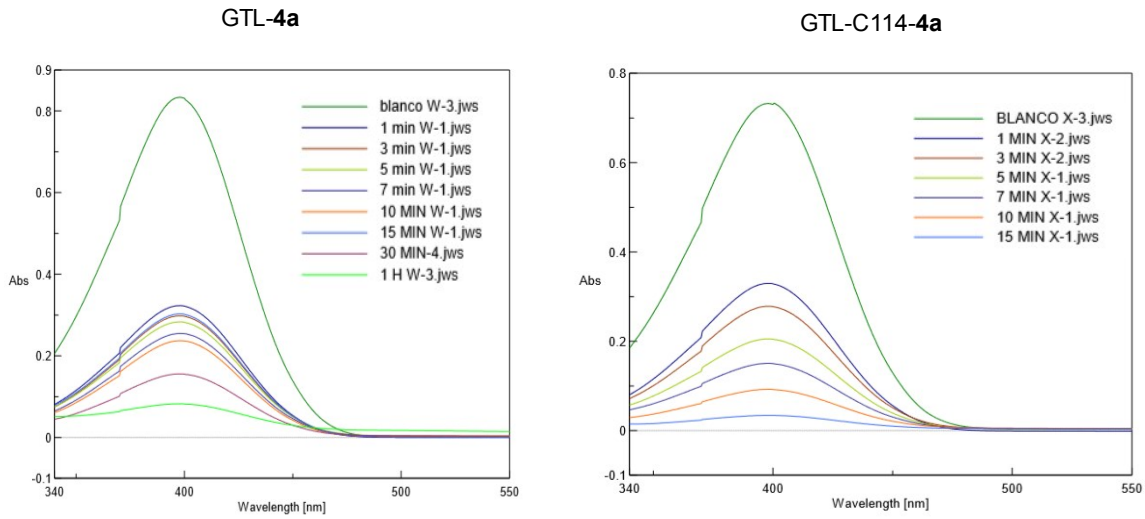

Figure S12. Time-dependent absorption spectra of the Pd-catalyzed reduction of pNP in the presence of different GTL variants-**4a** conjugates and $NaBH_4$.

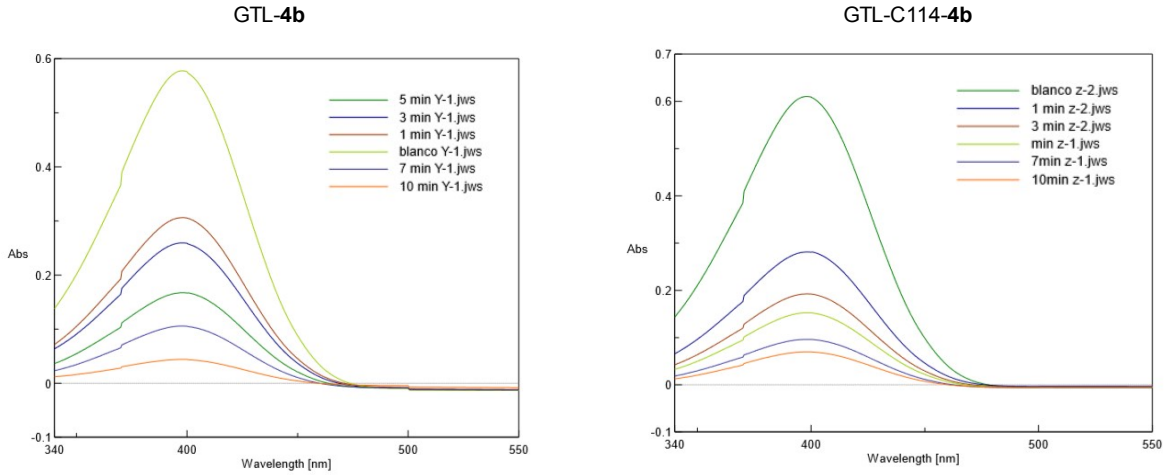

Figure S13. Time-dependent absorption spectra of the Pd-catalyzed reduction of pNP in the presence of different GTL variants-**4b** conjugates and $NaBH_4$.

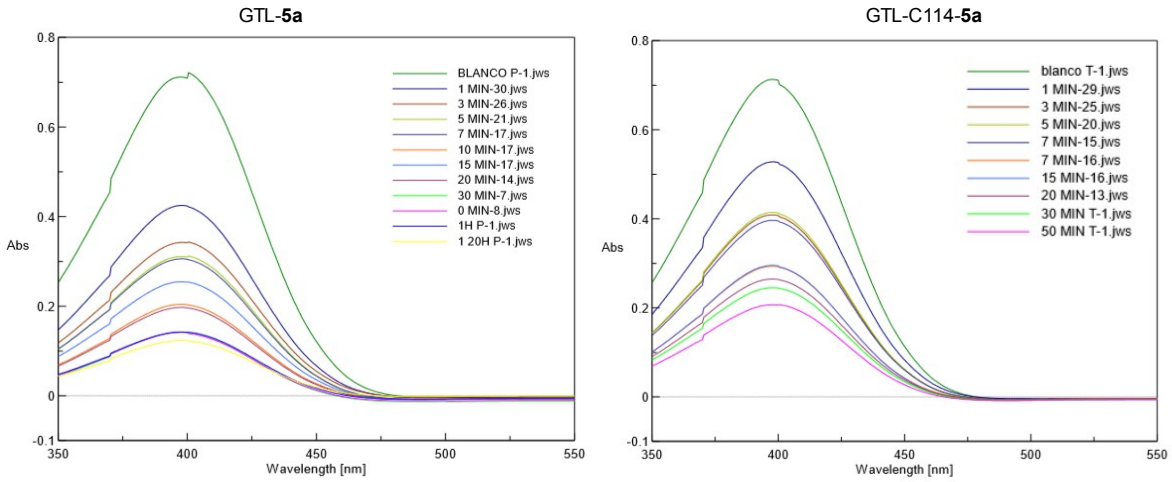

Figure S14. Time-dependent absorption spectra of the Pd-catalyzed reduction of pNP in the presence of different GTL variants-**5a** conjugates and $NaBH_4$.

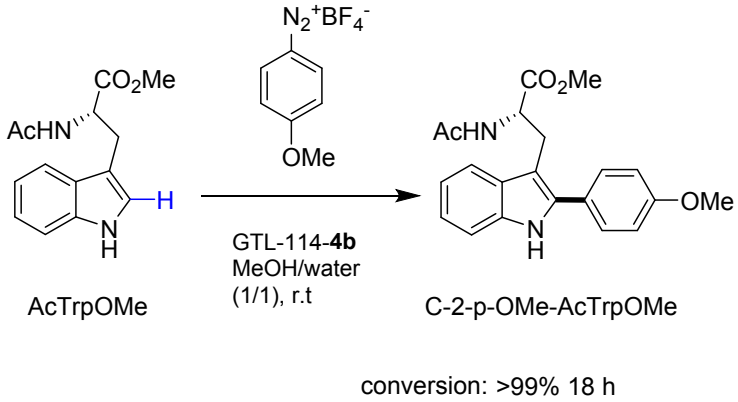

Figure S15. C-H arylation of AcTrpOMe catalysed by GTL114-**4b** conjugate in aqueous media and rt.

NMR and IR SPECTRA of Pd complexes

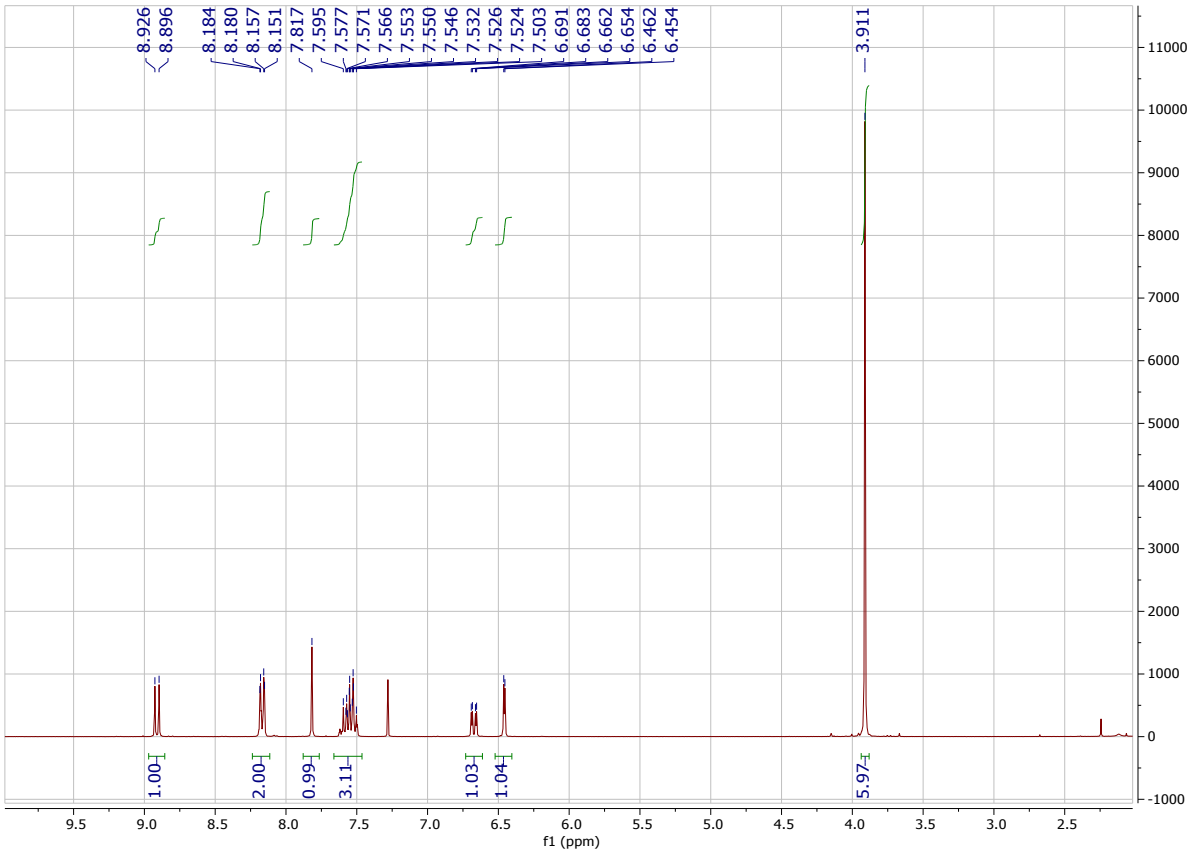

^{1}H NMR spectrum ($CDCl_3$, 300.13 MHz) of oxazolone **1a** (control spectrum)

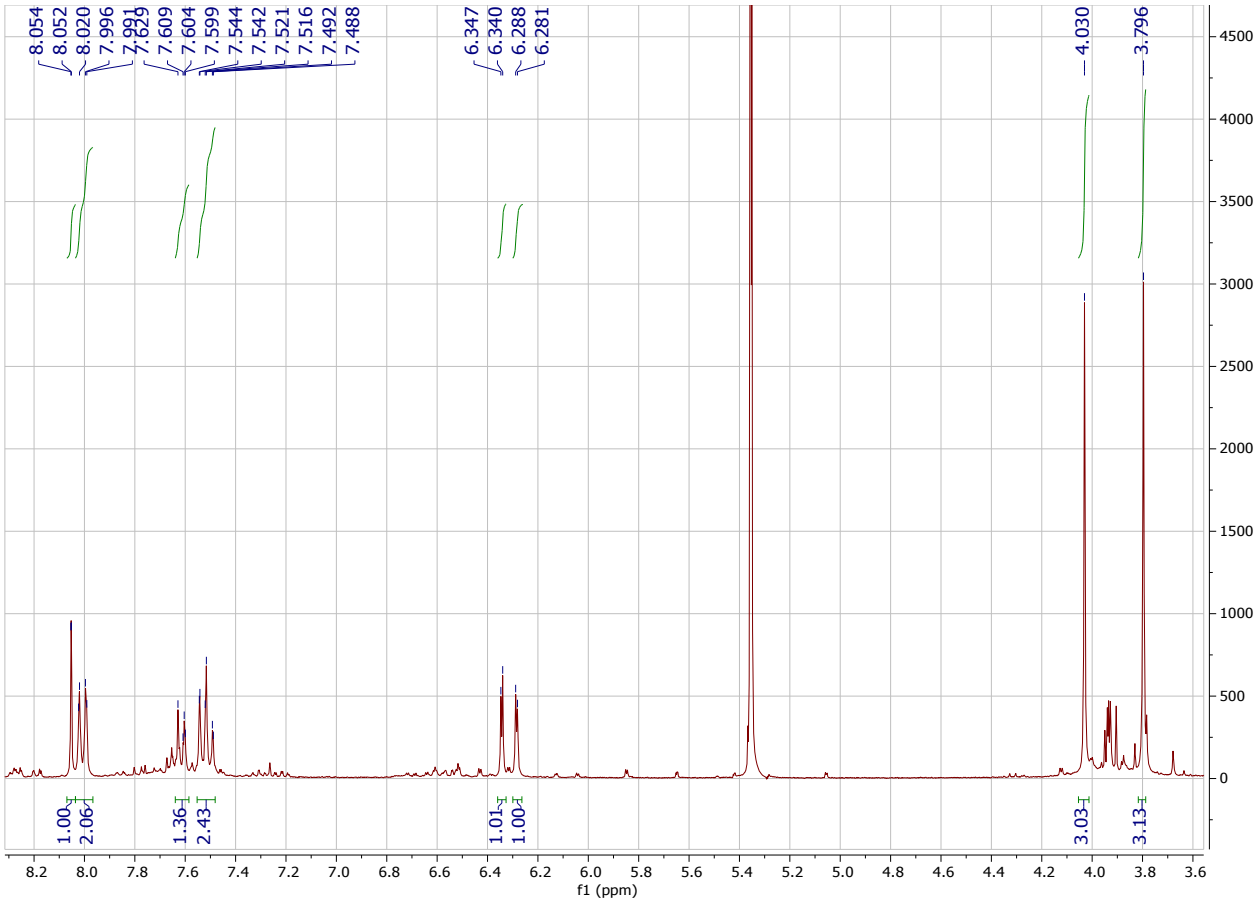

^{1}H NMR spectrum (CD_2Cl_2, 300.13 MHz) of orthopalladated **2a**

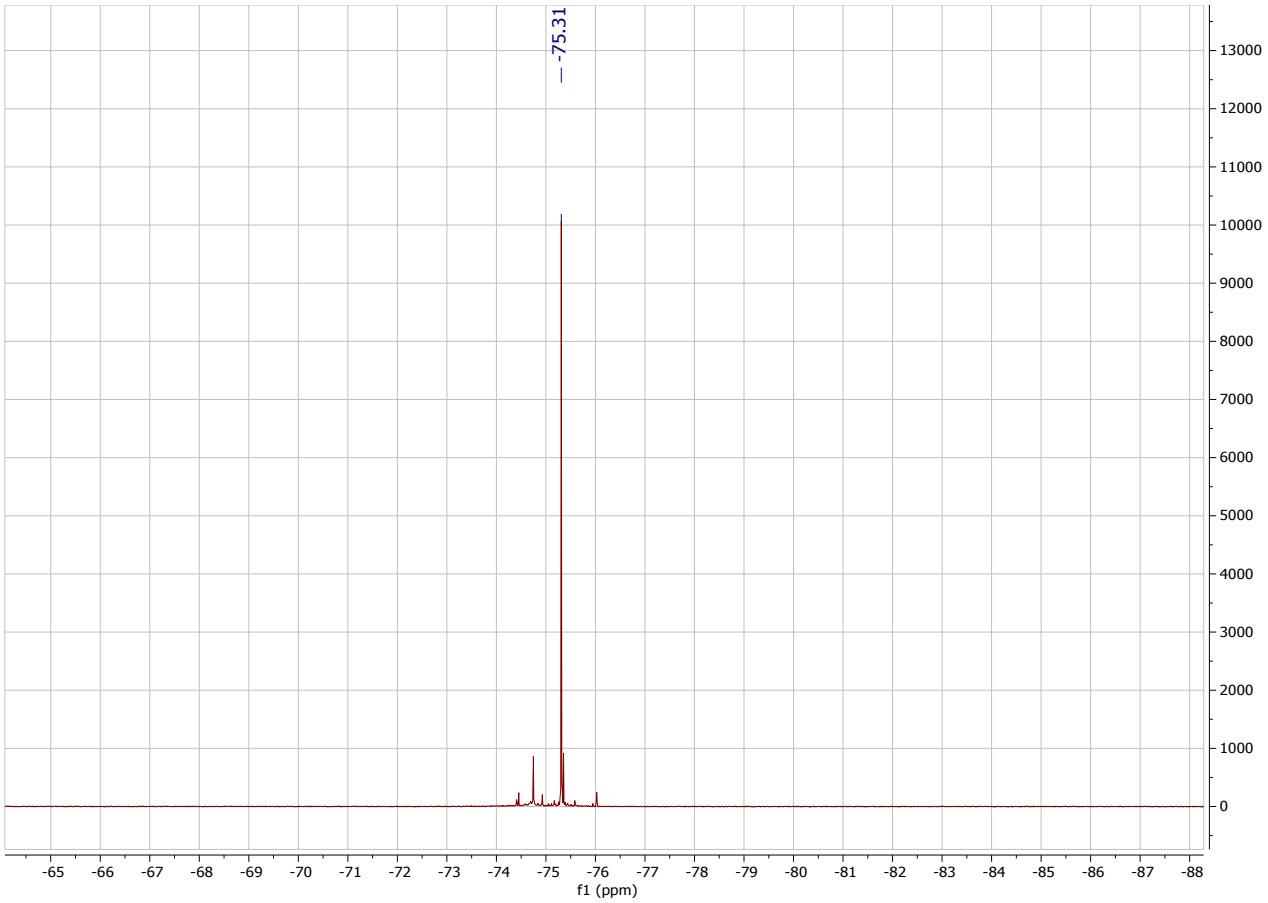

^{19}F NMR spectrum (CD_2Cl_2, 282.40 MHz) of orthopalladated **2a**

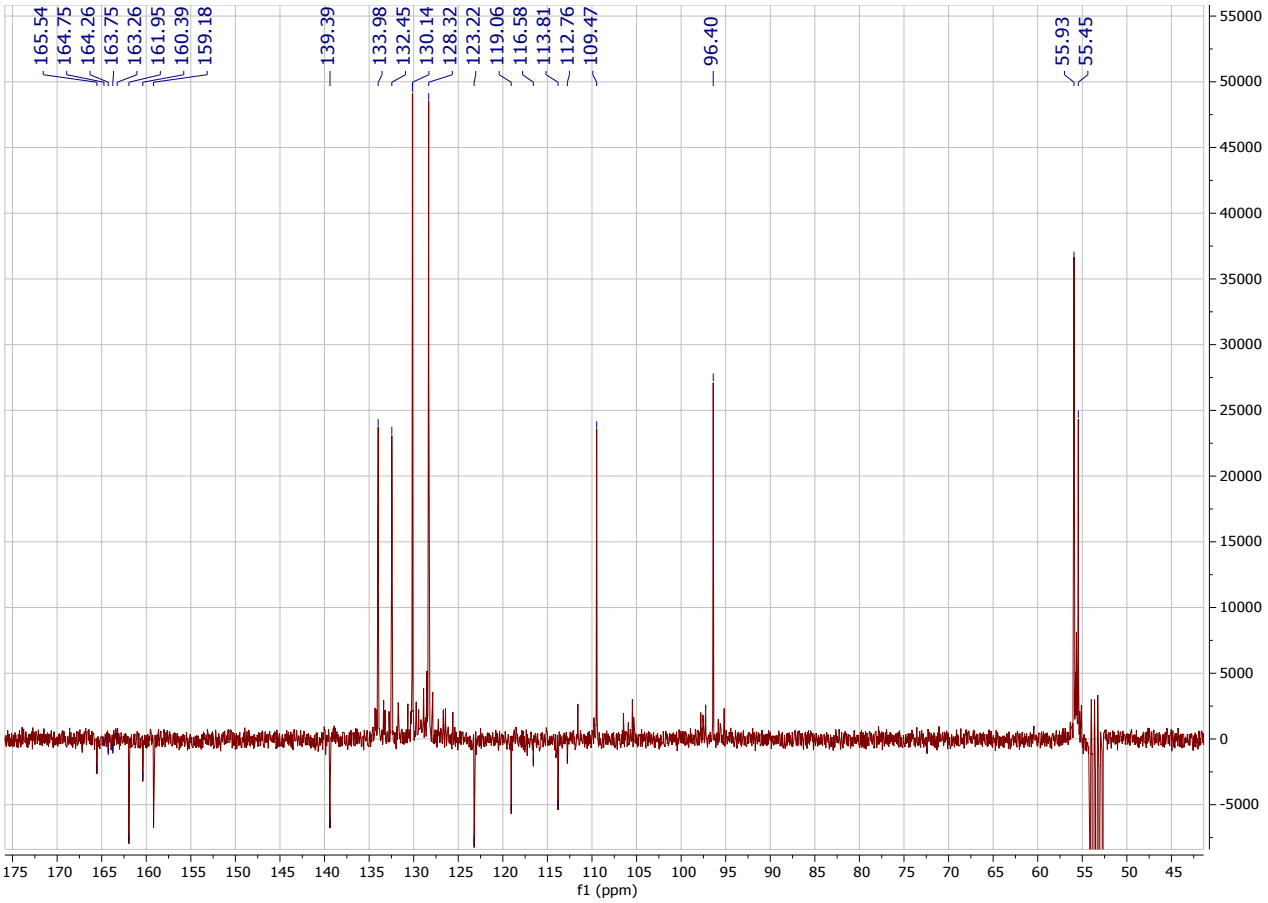

$^{13}C\{^{1}H\}$-APT NMR spectrum (CD_2Cl_2, 75.47 MHz) of orthopalladated **2a**

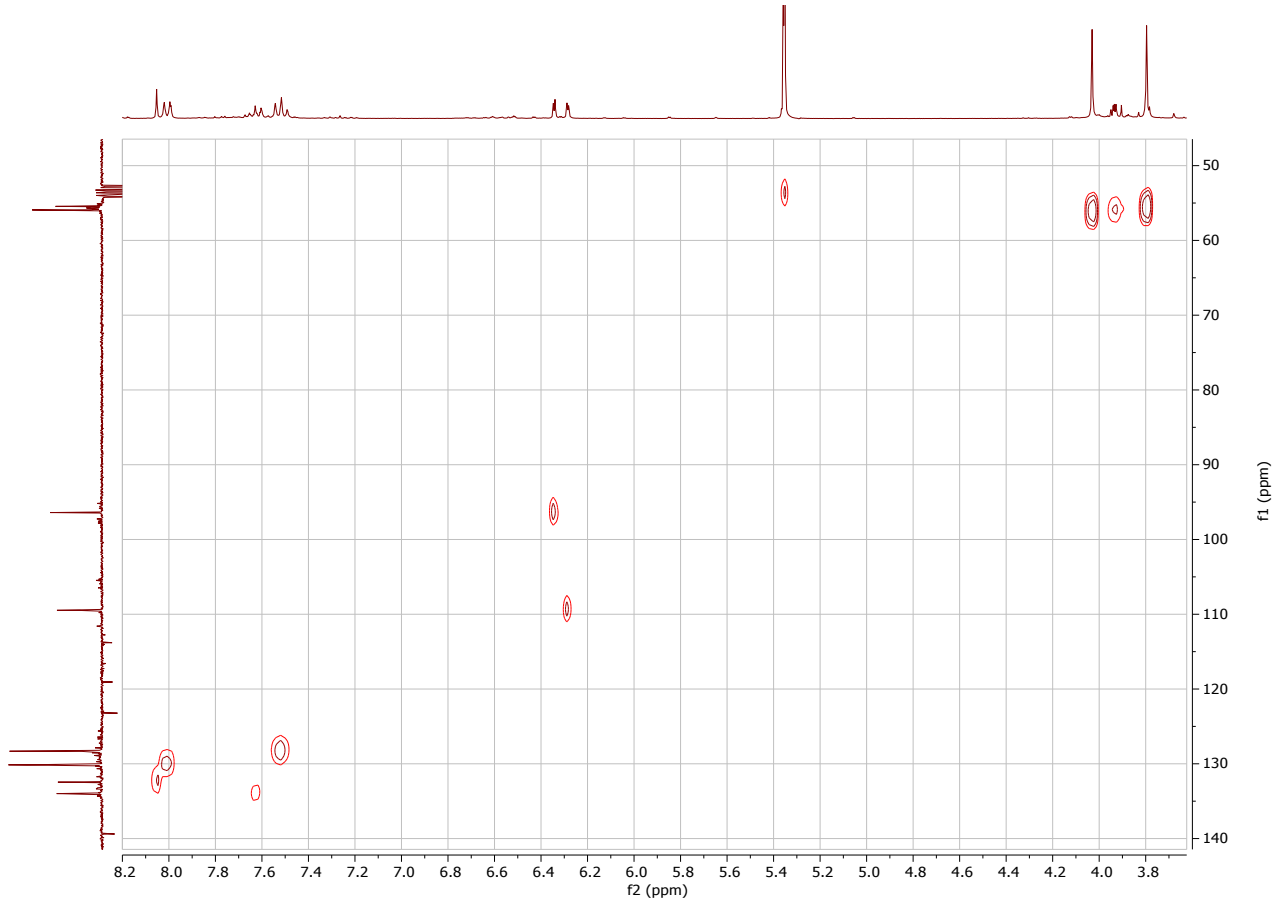

^{1}H-^{13}C HSQC correlation of orthopalladated **2a**

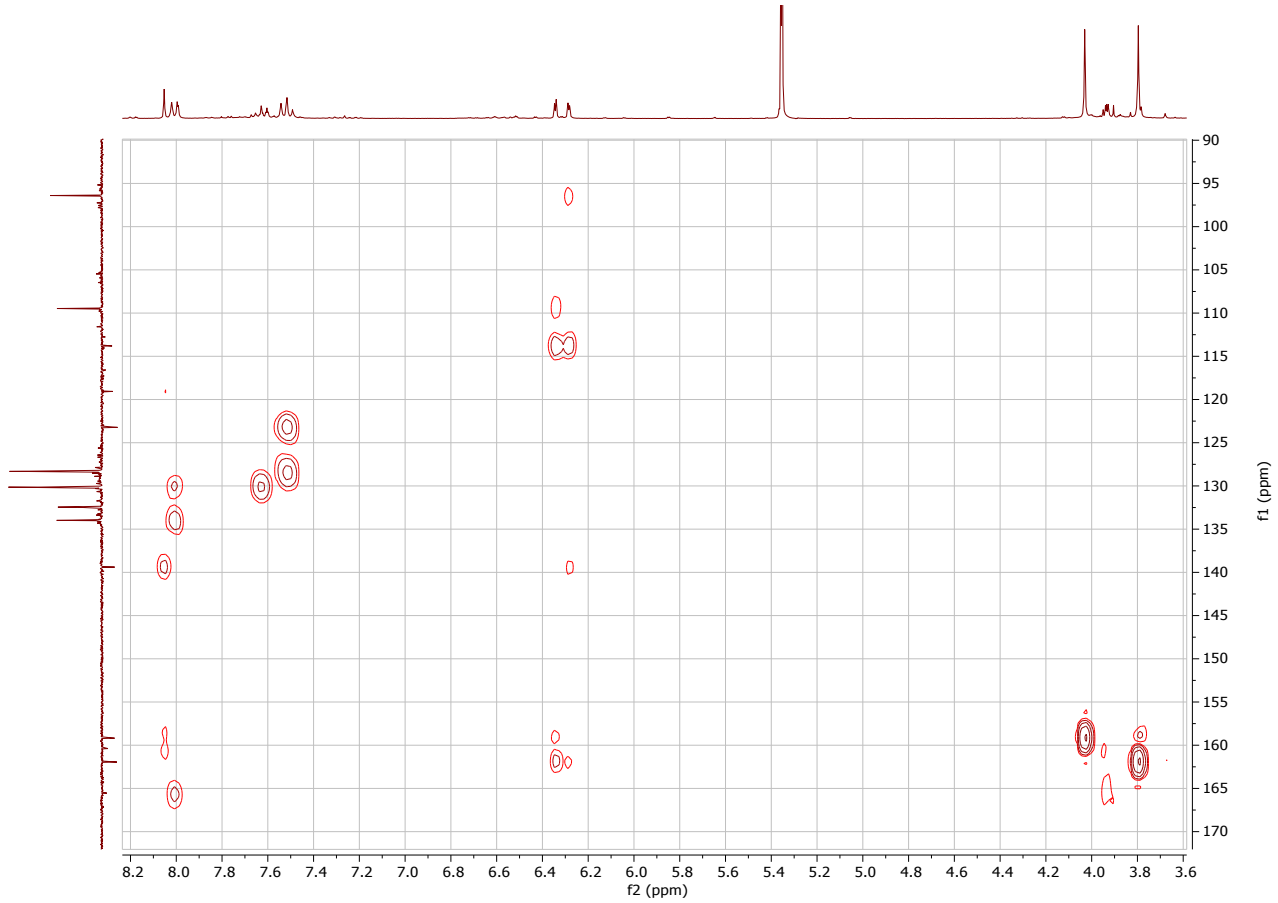

^{1}H-^{13}C HMBC correlation of orthopalladated **2a**

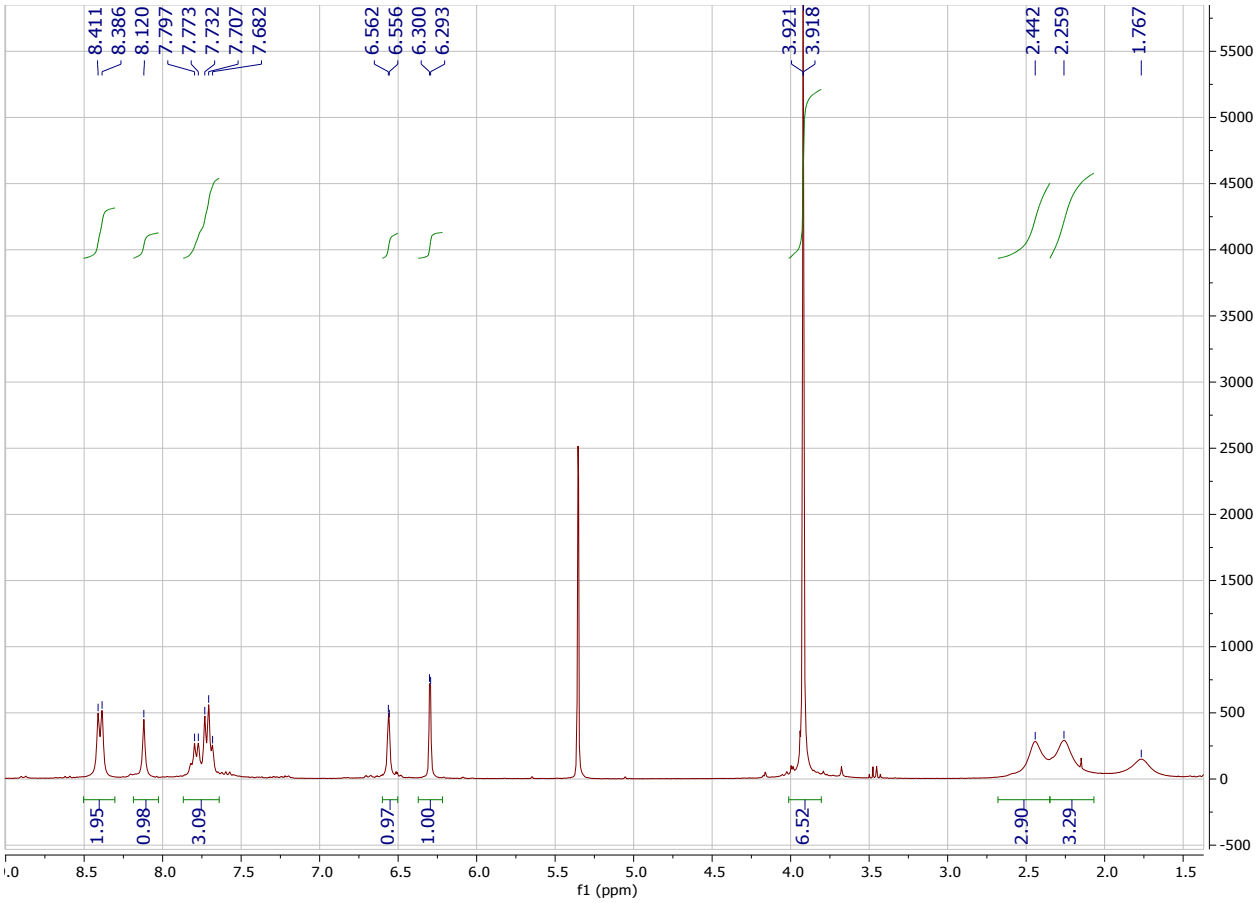

^{1}H NMR spectrum ($CDCl_3$, 300.13 MHz) of orthopalladated **4a**

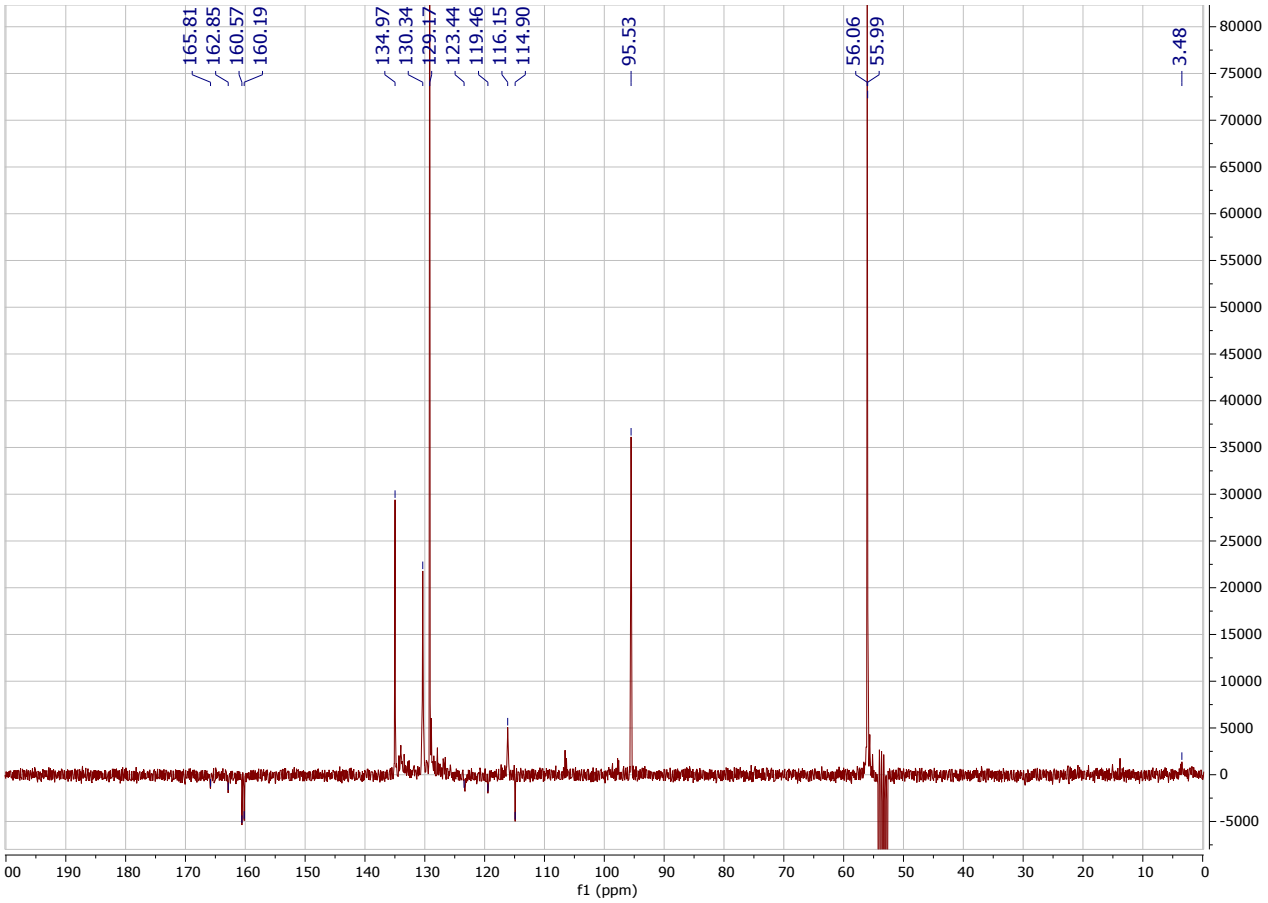

$^{13}C\{^{1}H\}$-APT NMR spectrum ($CDCl_3$, 75.47 MHz) of orthopalladated **4a**

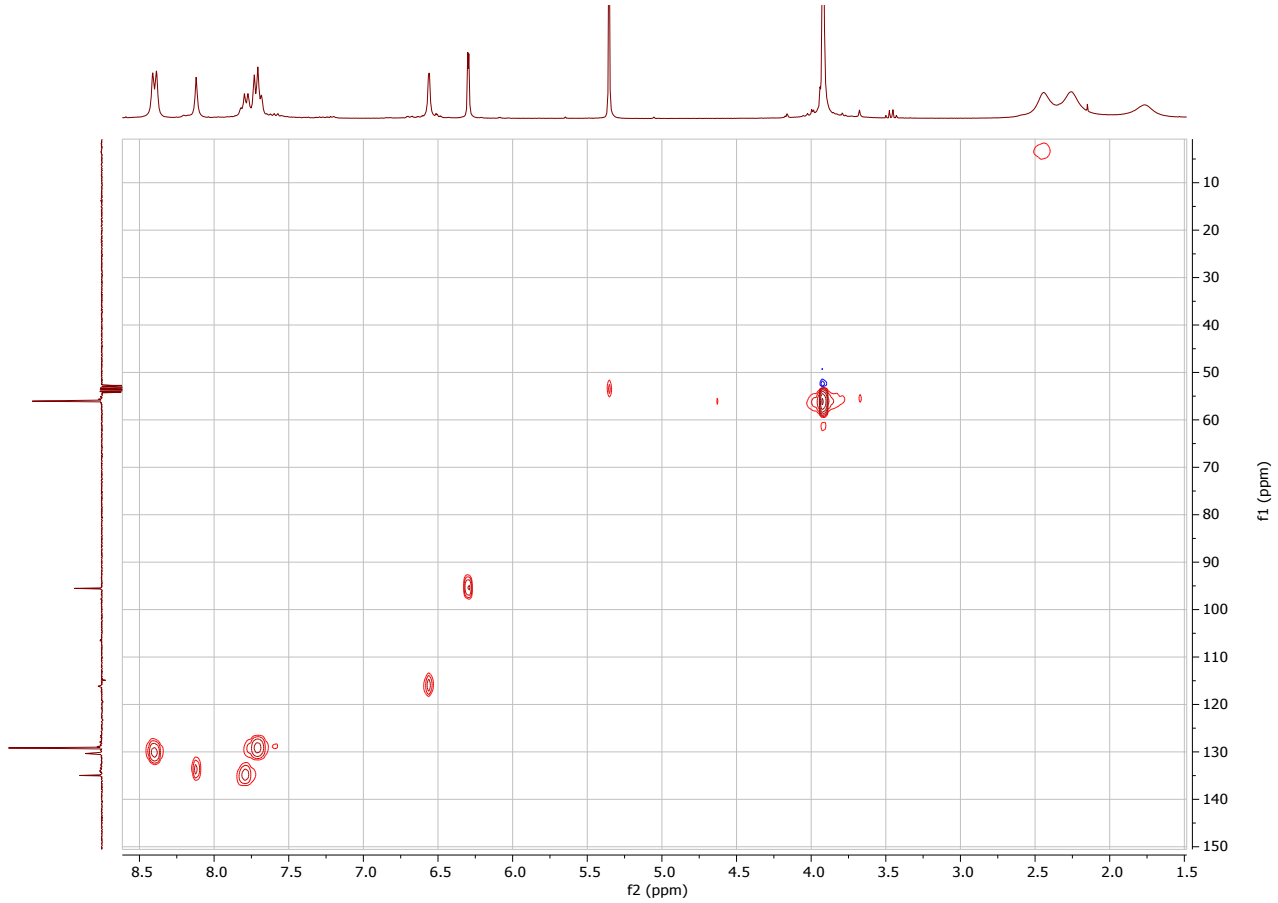

^{1}H-^{13}C HSQC correlation of orthopalladated **4a**

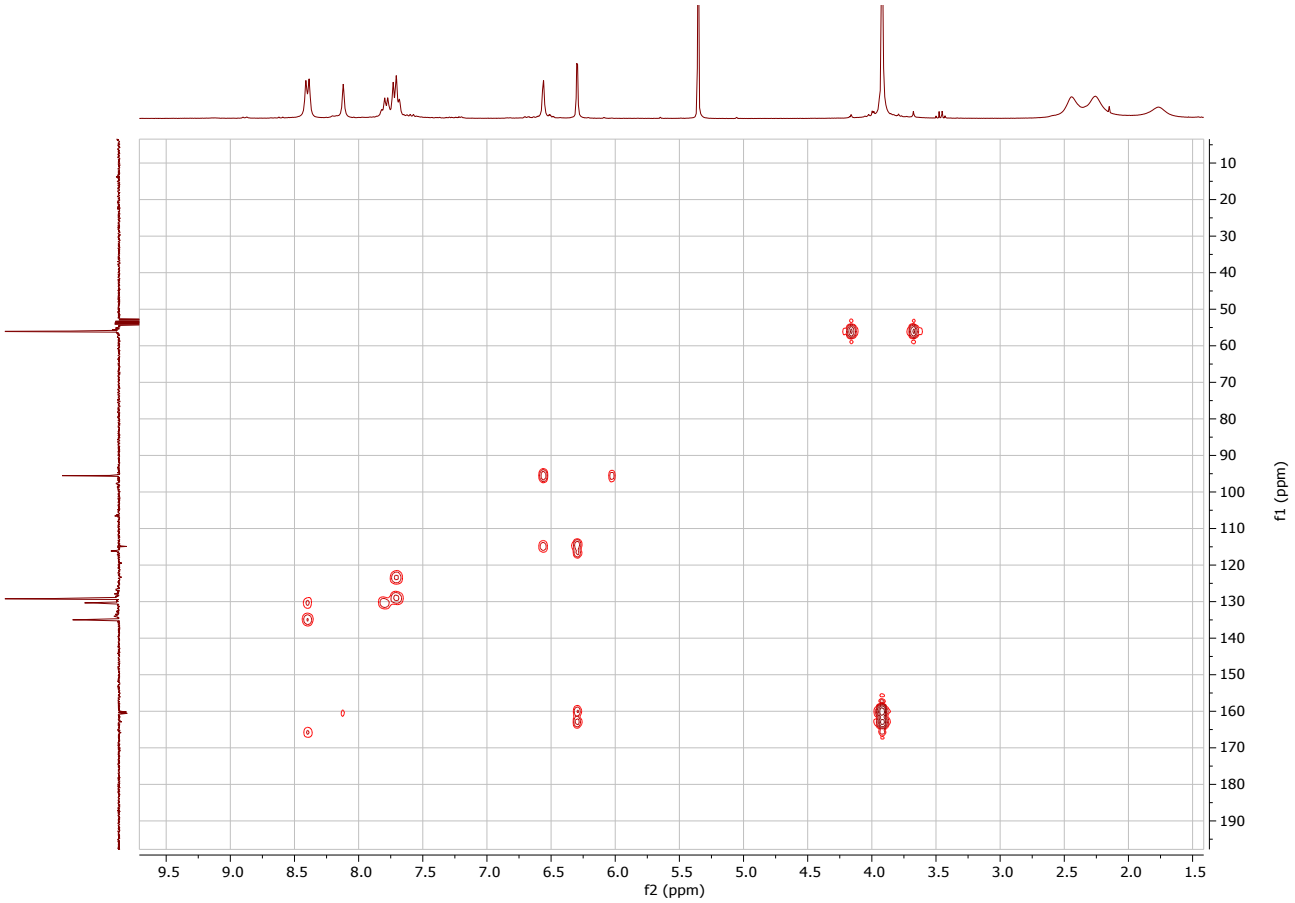

^{1}H-^{13}C HMBC correlation of orthopalladated **4a**

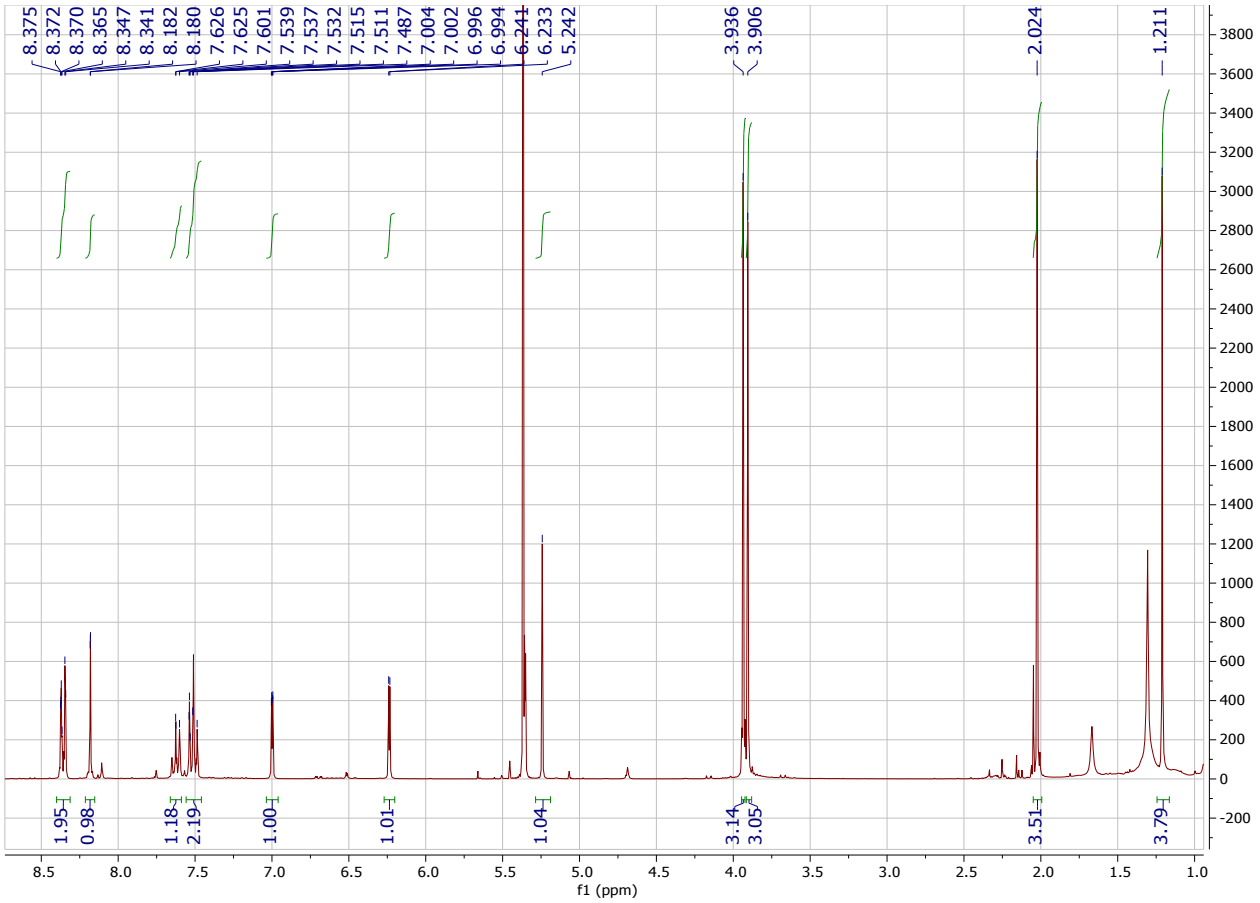

^{1}H NMR spectrum (CD_2Cl_2, 300.13 MHz) of orthopalladated **5a**

^{1}H NMR spectrum (CD_2Cl_2, 300.13 MHz) of orthopalladated **5a** (zoom aromatic region)

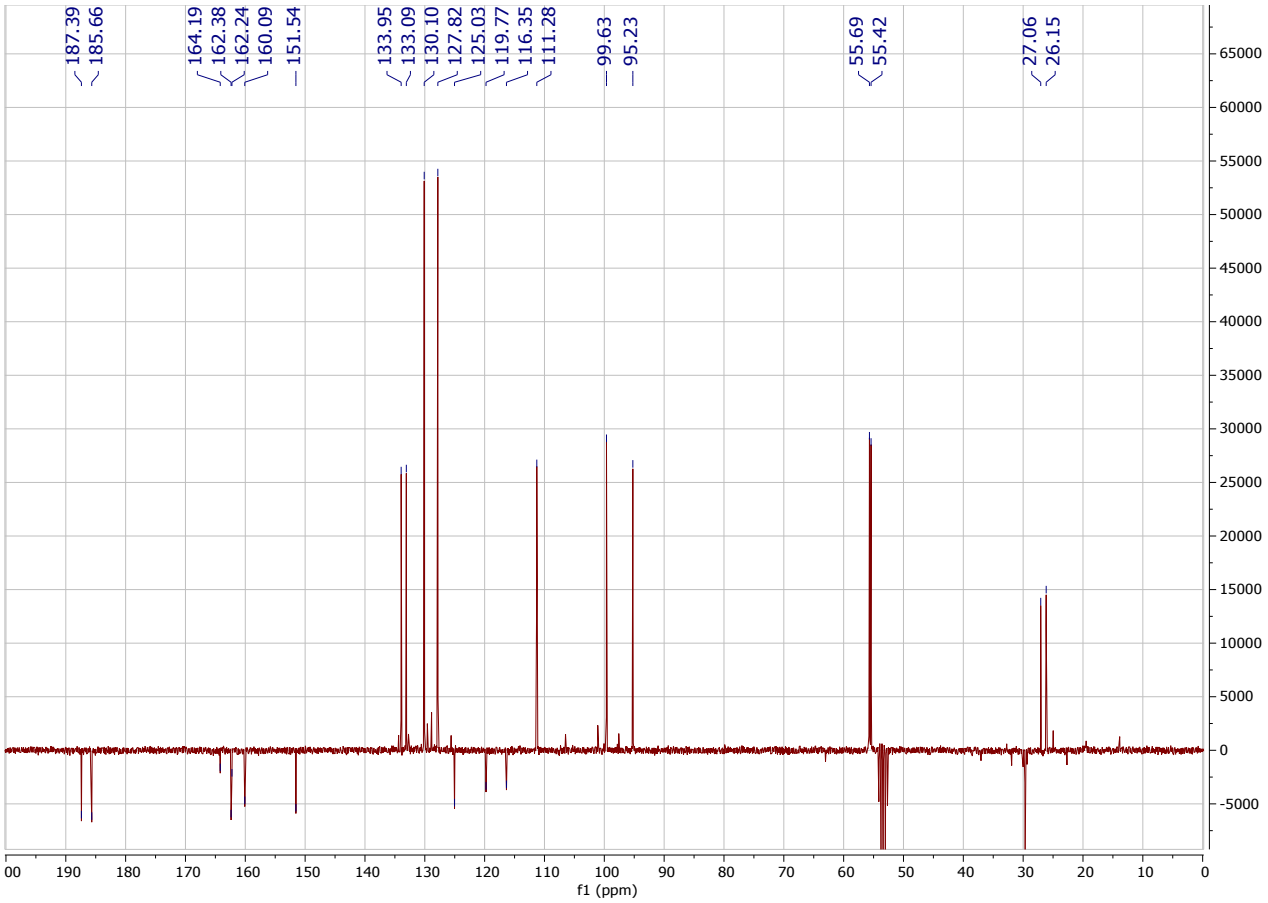

$^{13}C\{^{1}H\}$-APT NMR spectrum (CD_2Cl_2, 75.47 MHz) of orthopalladated **5a**

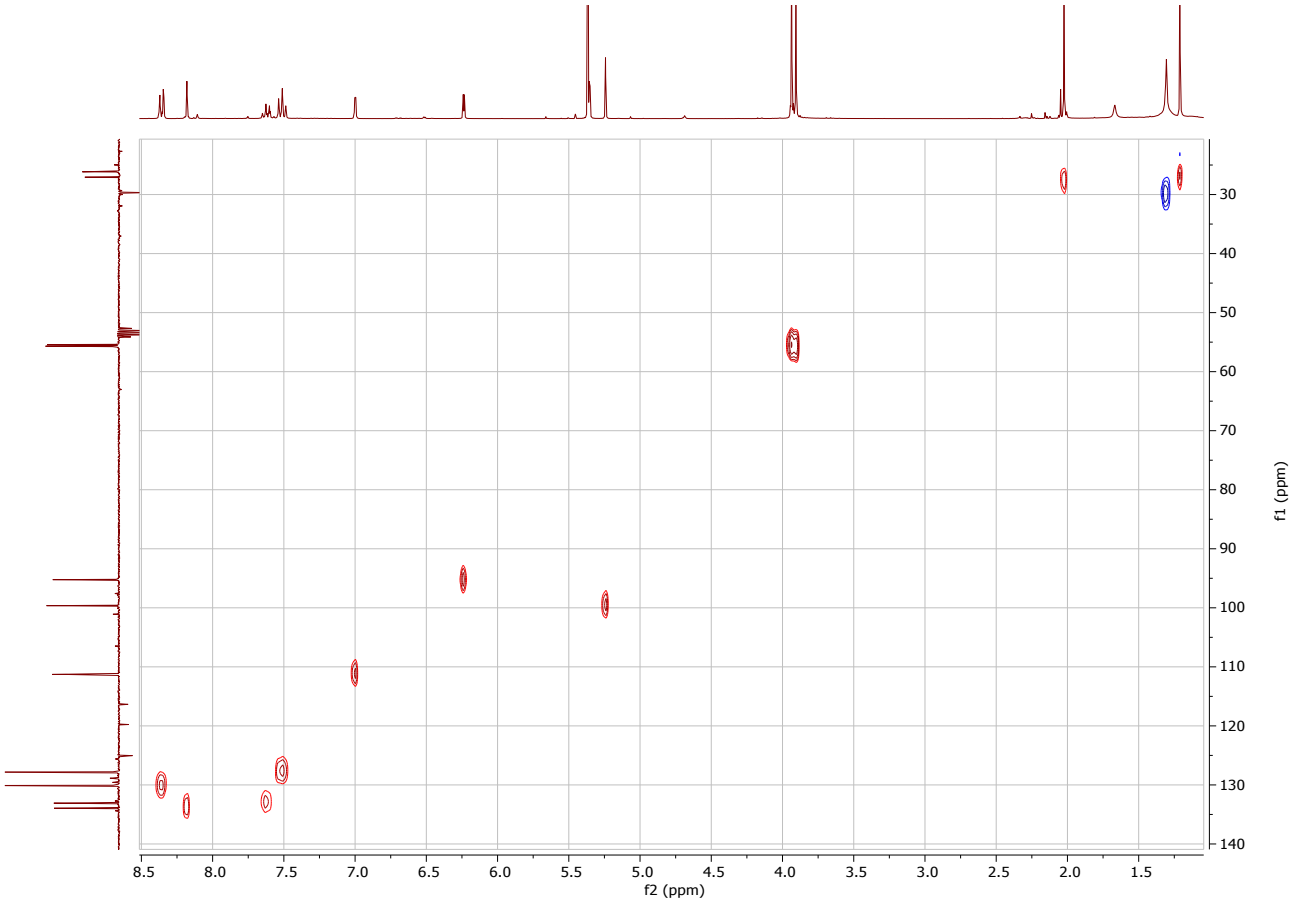

^{1}H-^{13}C HSQC correlation of orthopalladated **5a**

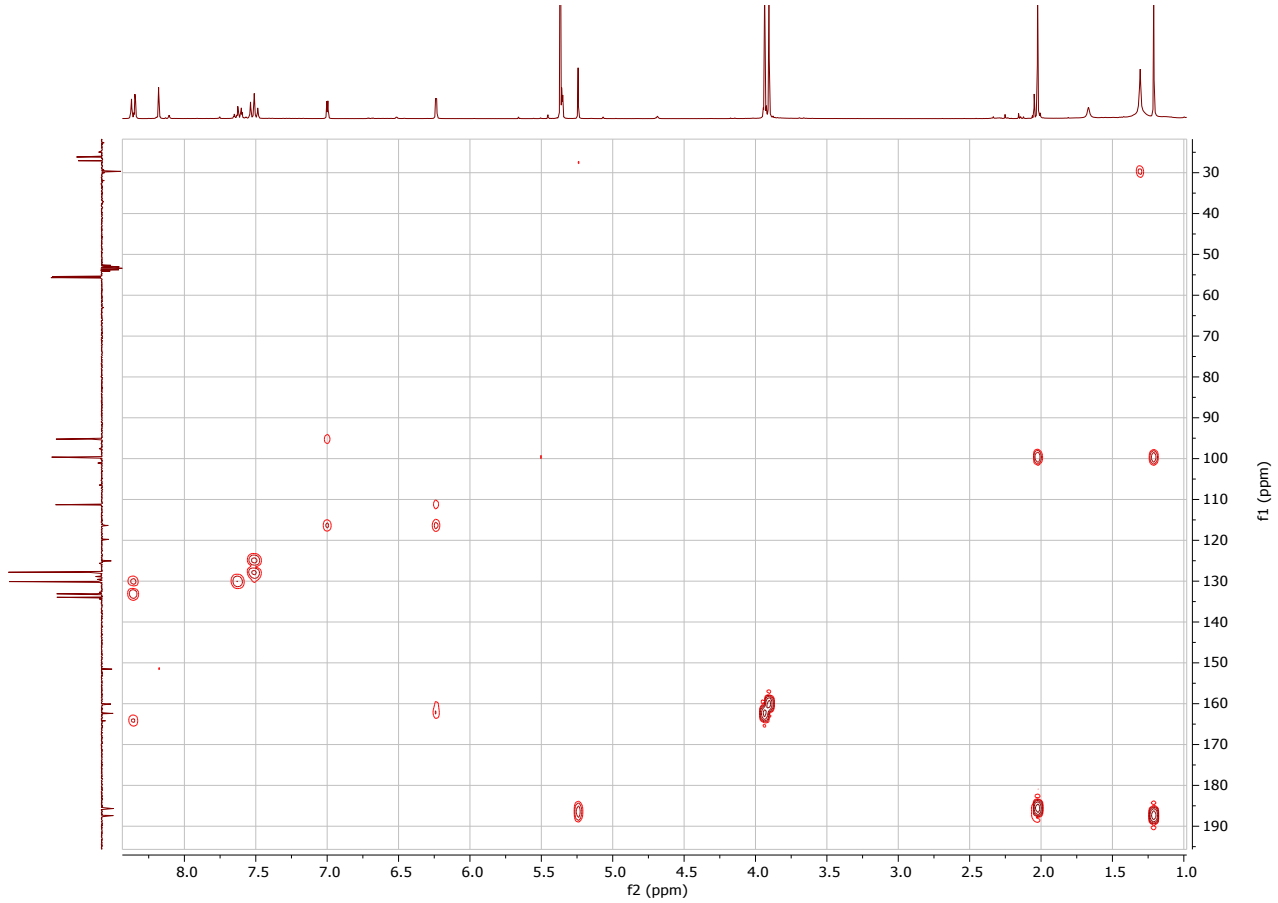

^{1}H-^{13}C HMBC correlation of orthopalladated **5a**

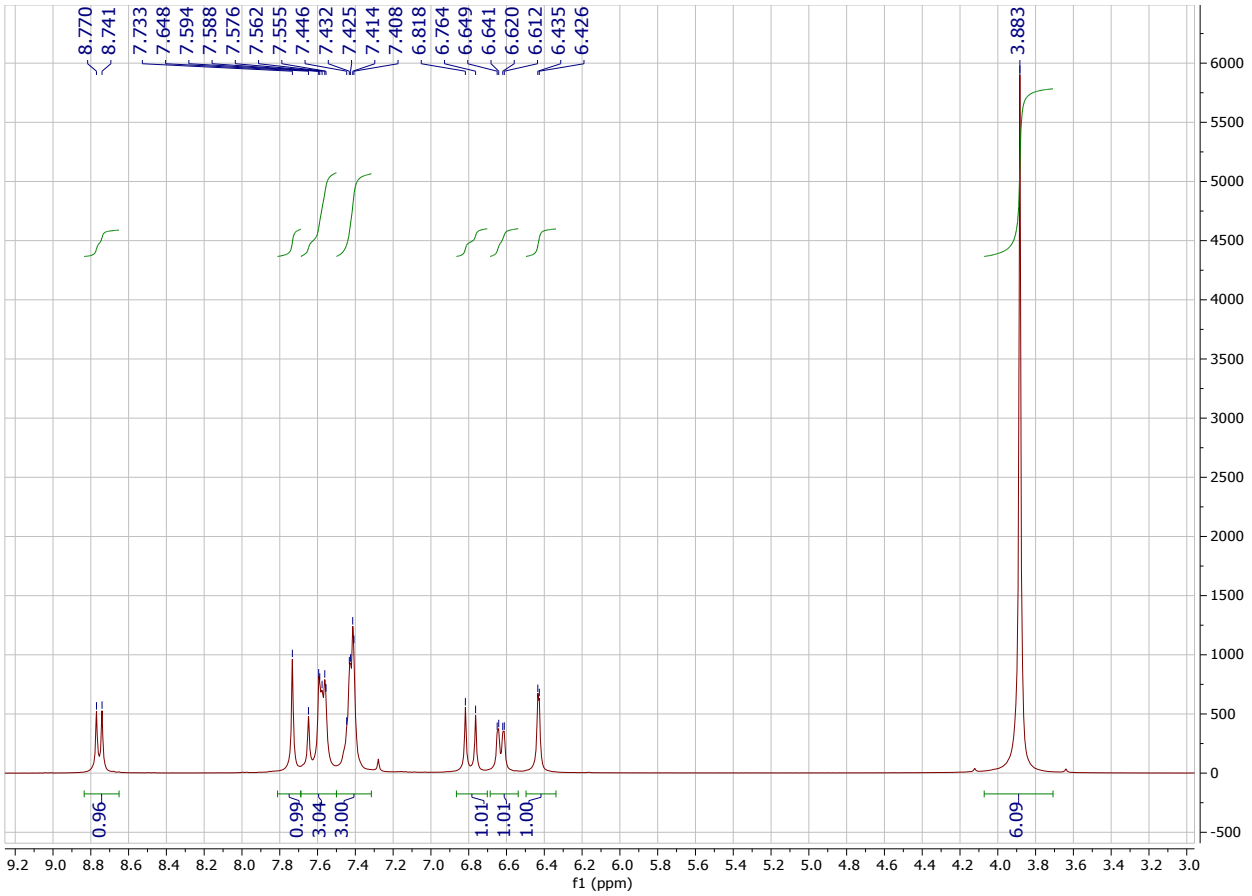

^{1}H-NMR spectrum ($CDCl_3$, 300.13 MHz) of oxazolone **1b**

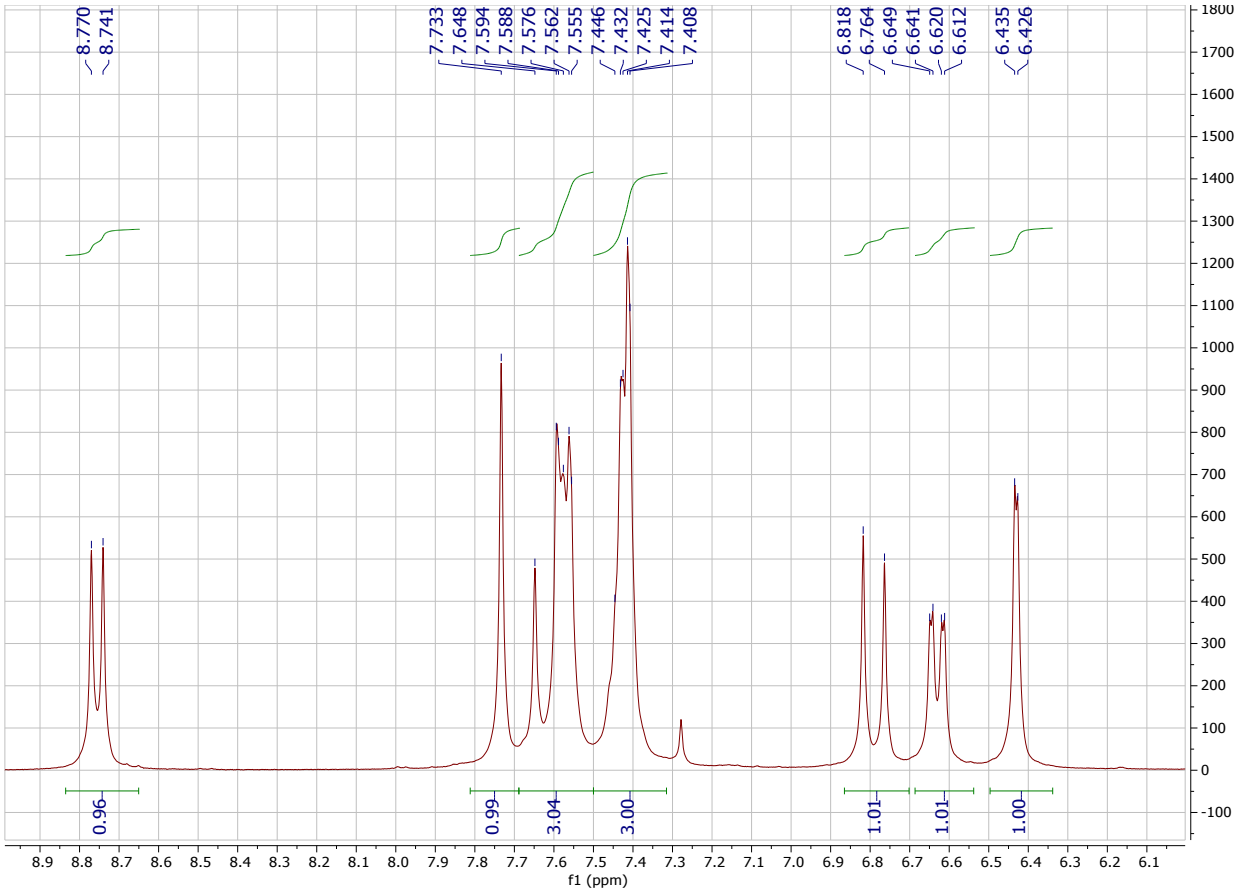

^{1}H-NMR spectrum ($CDCl_3$, 300.13 MHz) of oxazolone **1b**, zoom aromatic region

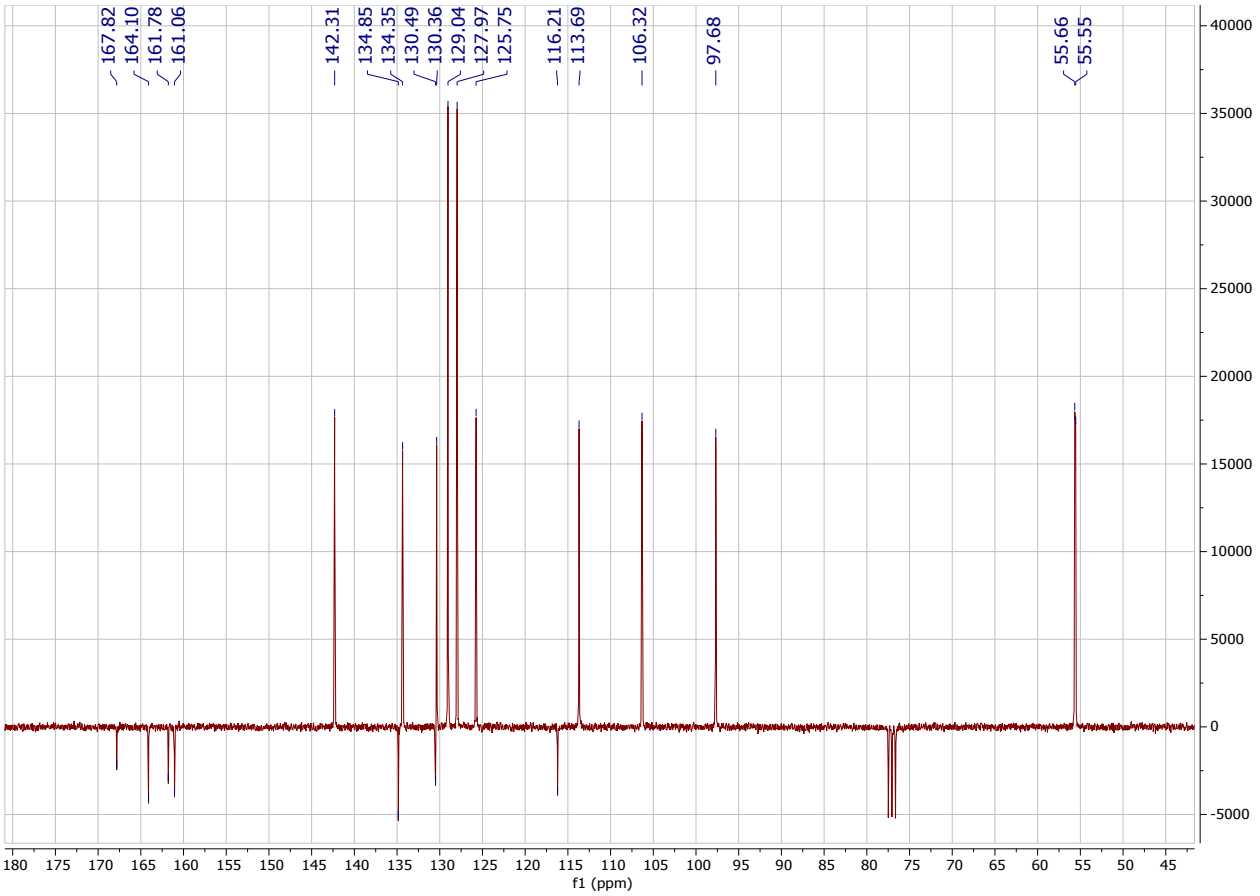

$^{13}C\{^{1}H\}$ (APT) NMR spectrum ($CDCl_3$, 75.47 MHz) of oxazolone **1b**

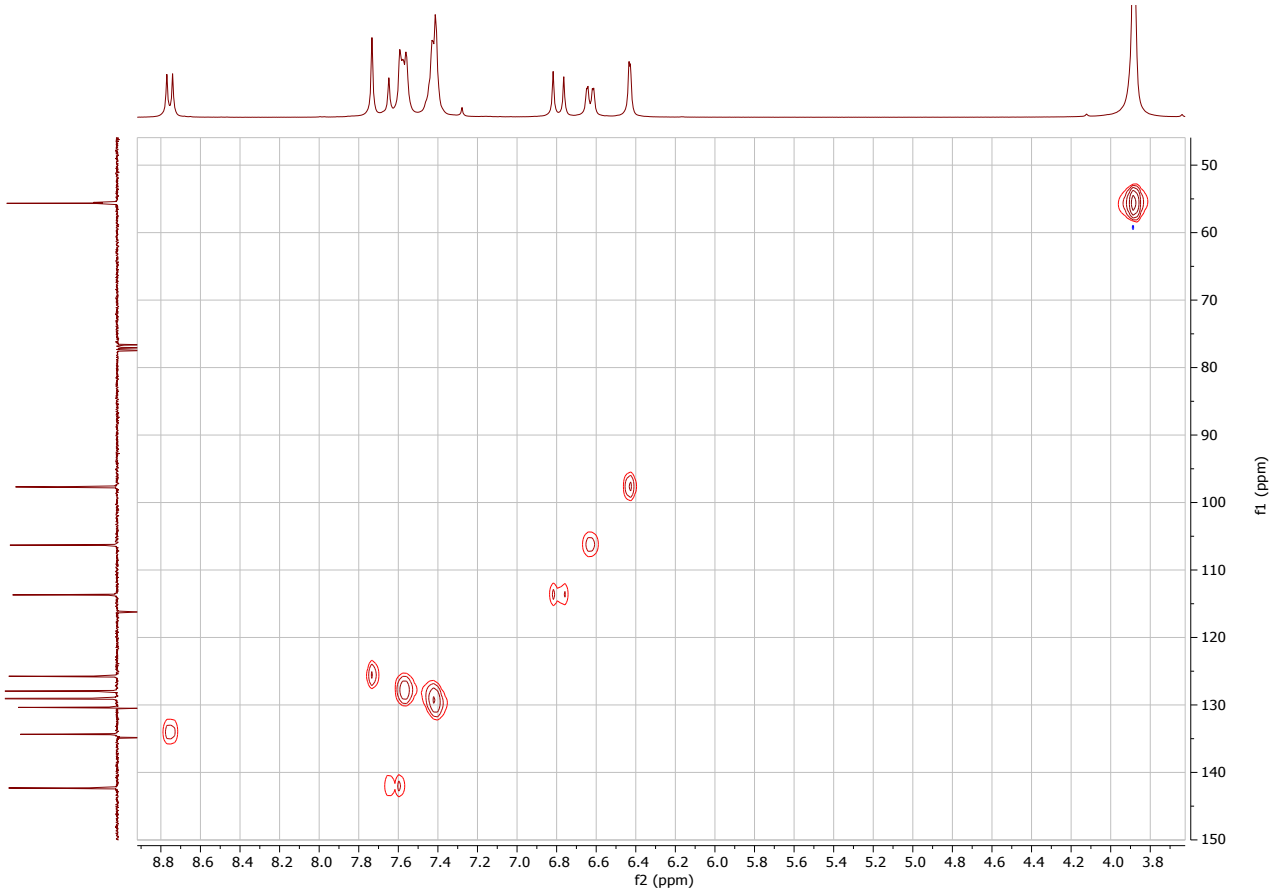

^{1}H-^{13}C HSQC correlation spectrum of oxazolone **1b**

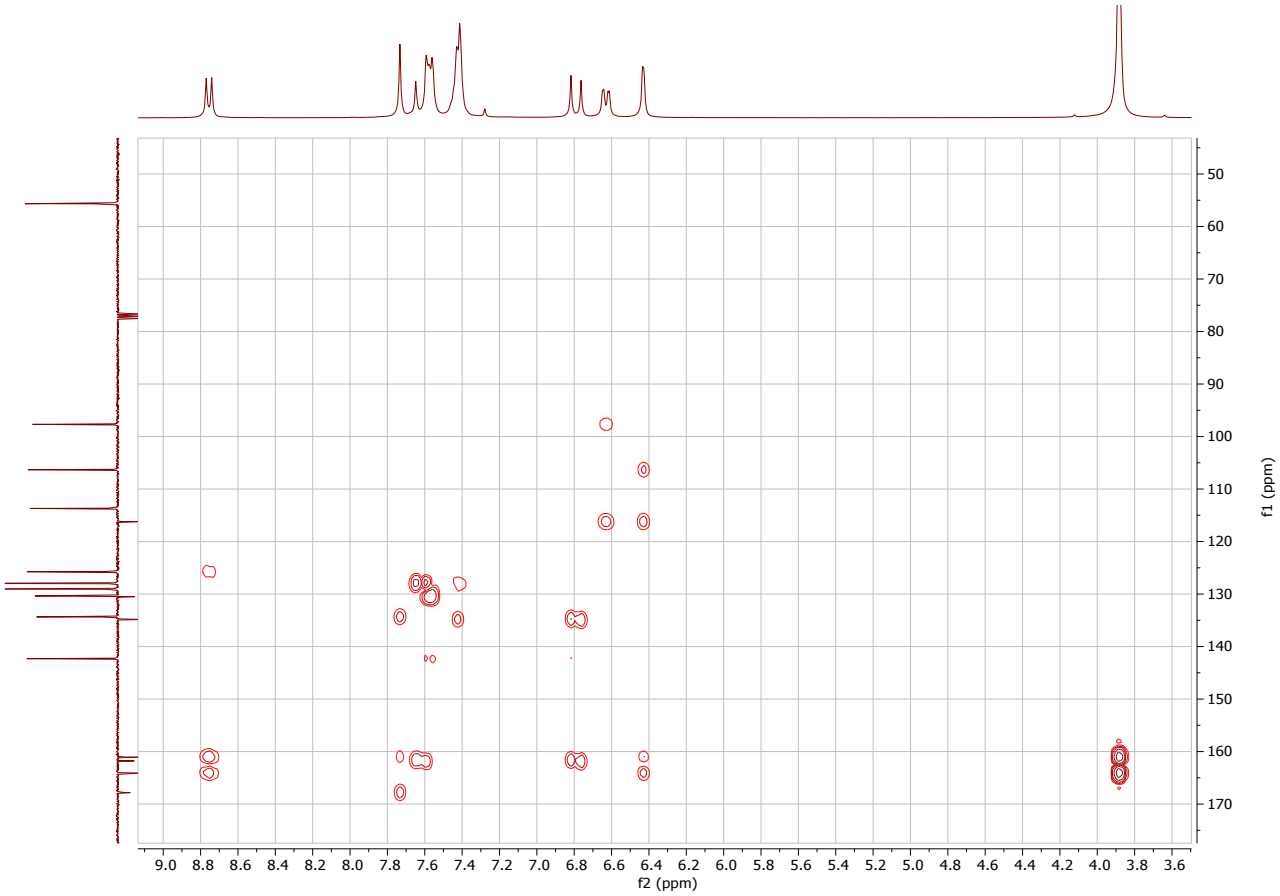

^{1}H-^{13}C HMBC correlation spectrum of oxazolone **1b**

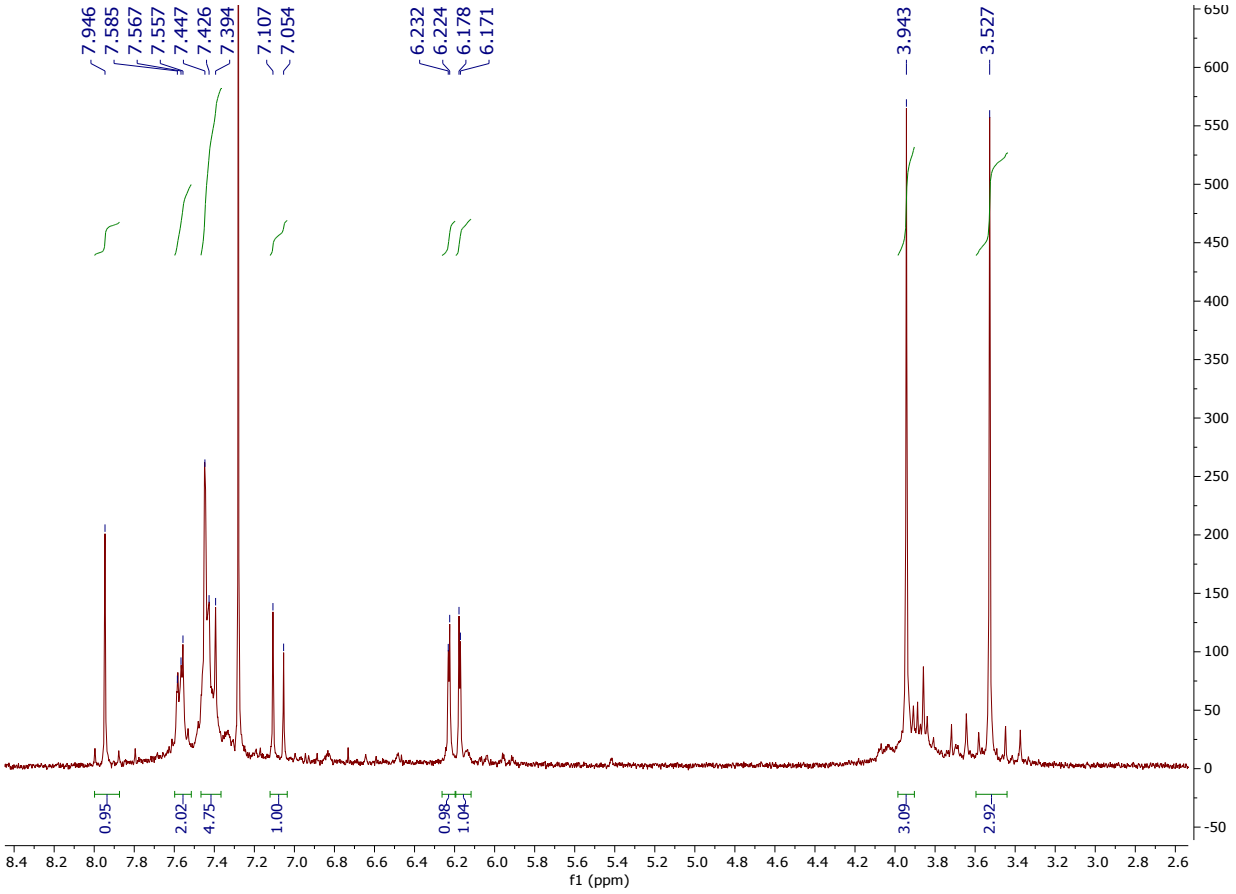

^{1}H-NMR spectrum ($CDCl_3$, 300.13 MHz) of orthopalladated **2b**

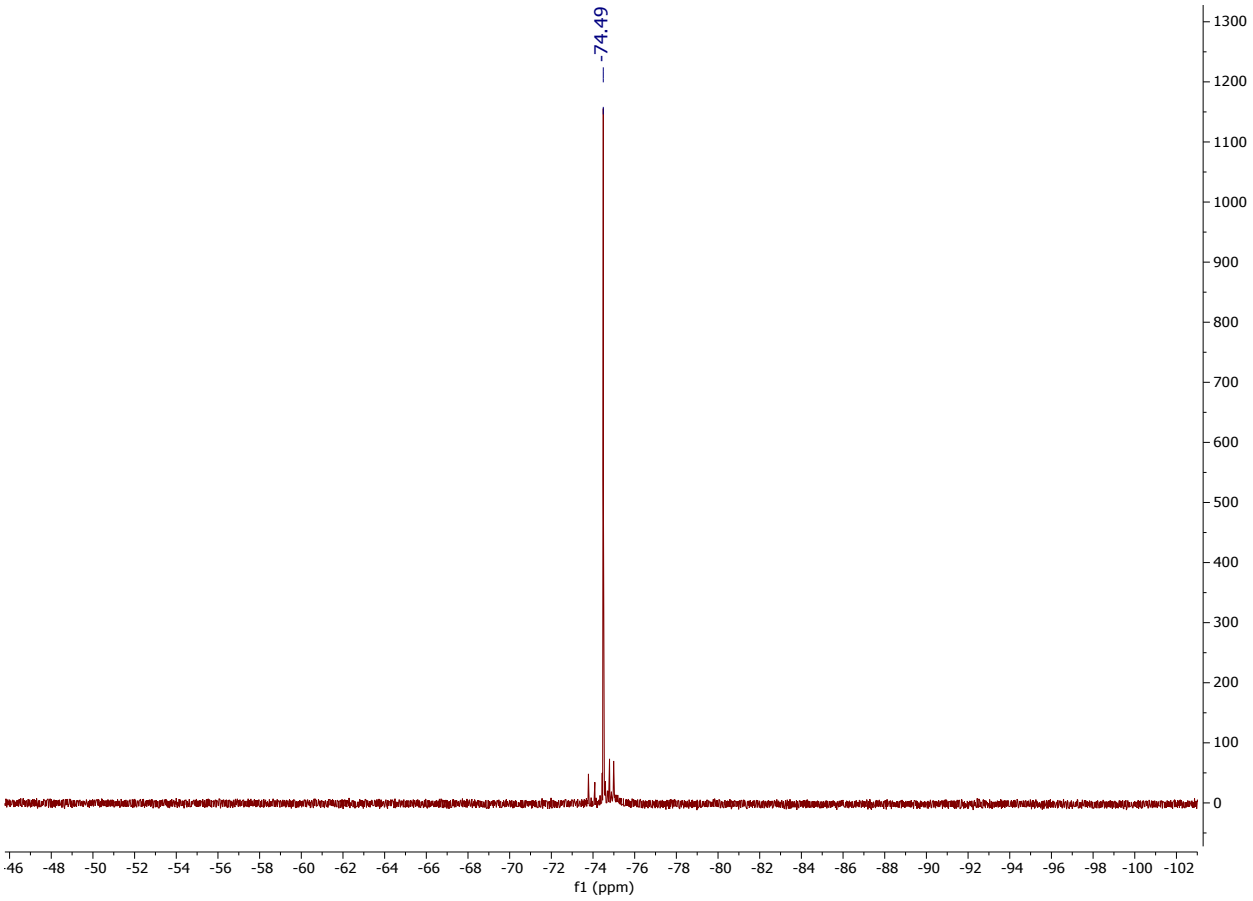

^{19}F-NMR spectrum ($CDCl_3$, 282.40 MHz) of orthopalladated **2b**

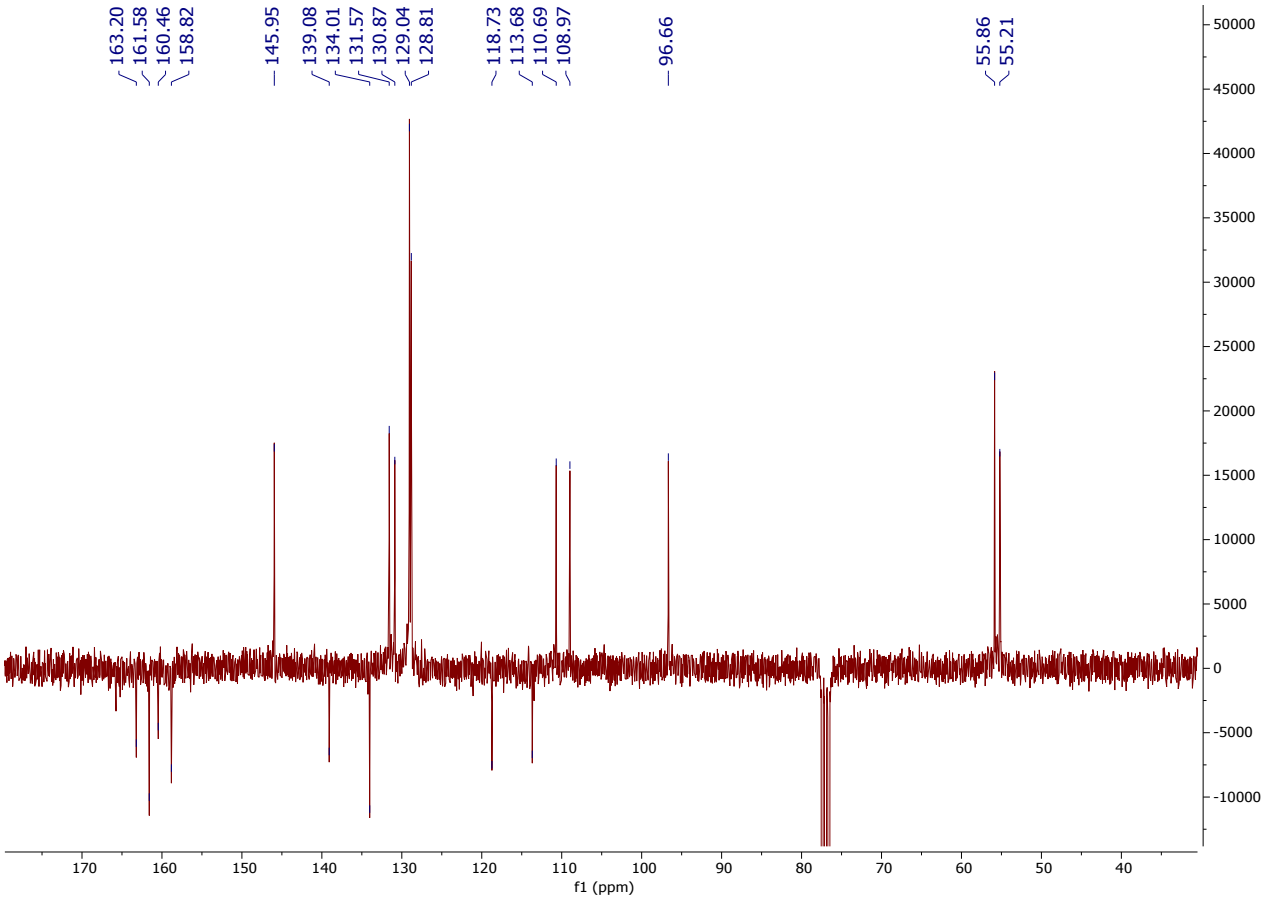

$^{13}C\{^{1}H\}$-(APT) NMR spectrum ($CDCl_3$, 75.47 MHz) of orthopalladated **2b**

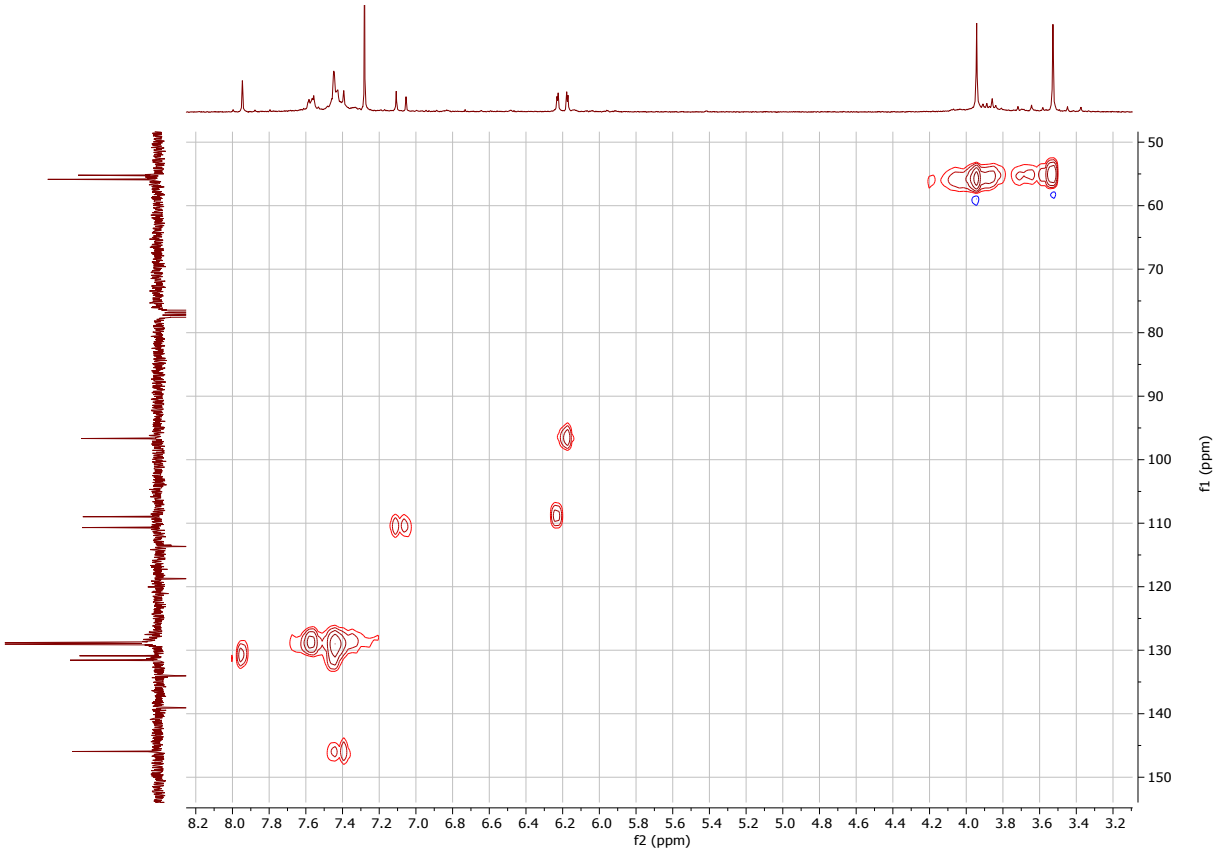

^{1}H-^{13}C HSQC correlation spectrum of orthopalladated **2b**

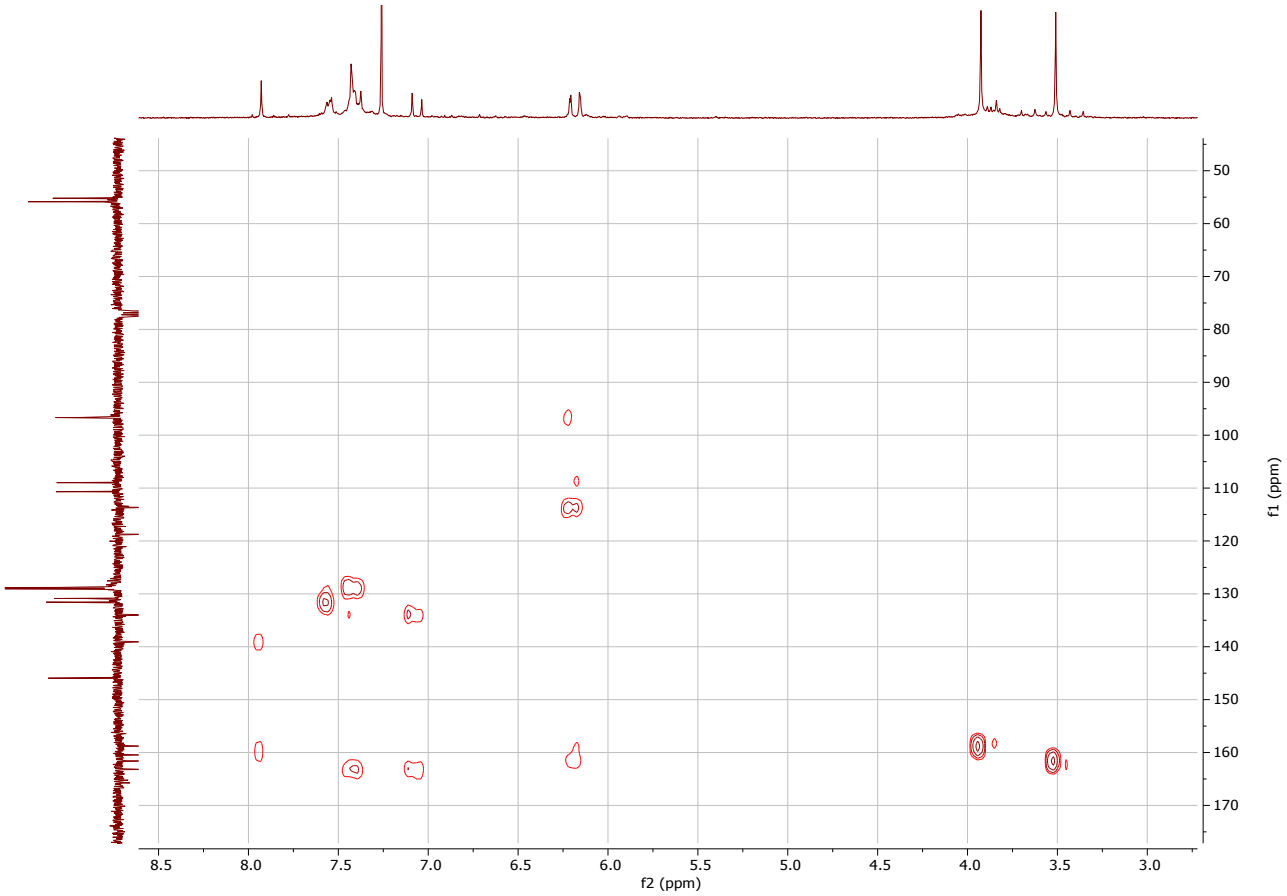

^{1}H-^{13}C HMBC correlation spectrum of orthopalladated **2b**

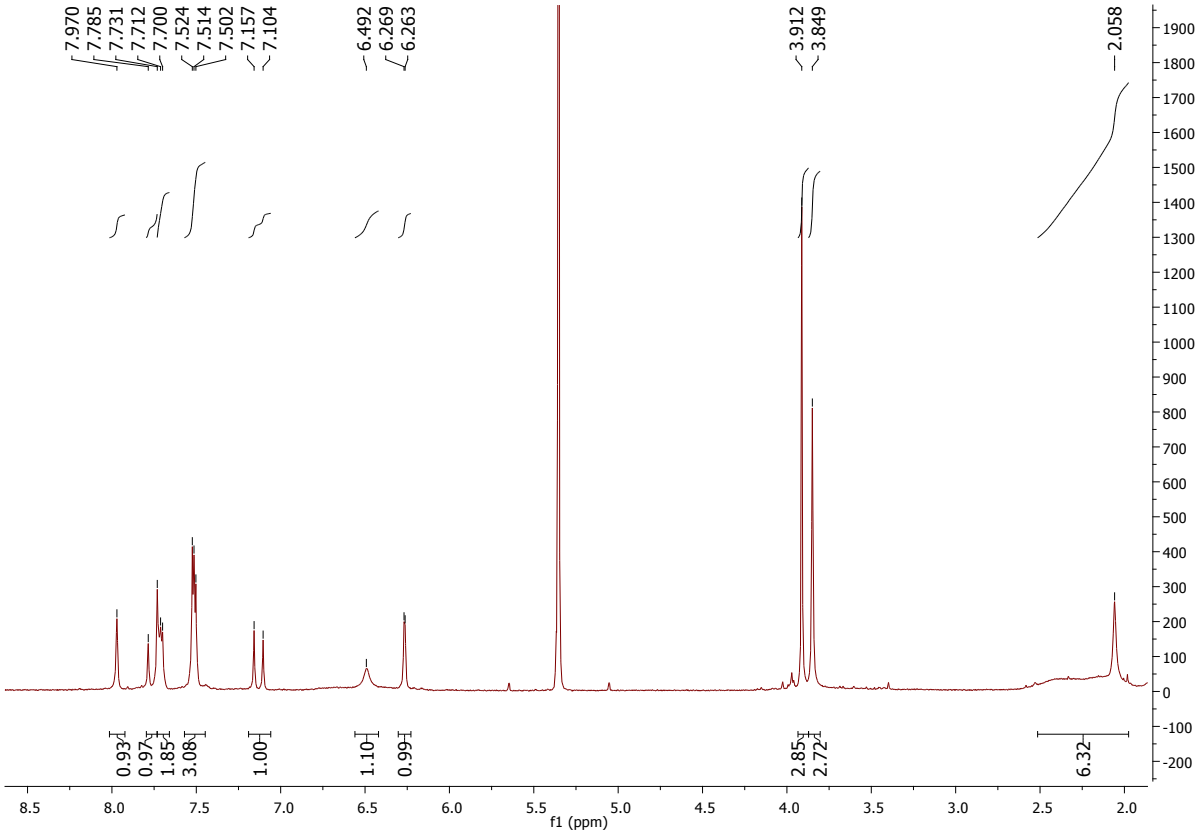

^{1}H-NMR spectrum (CD_2Cl_2, 300.13 MHz) of **4b**

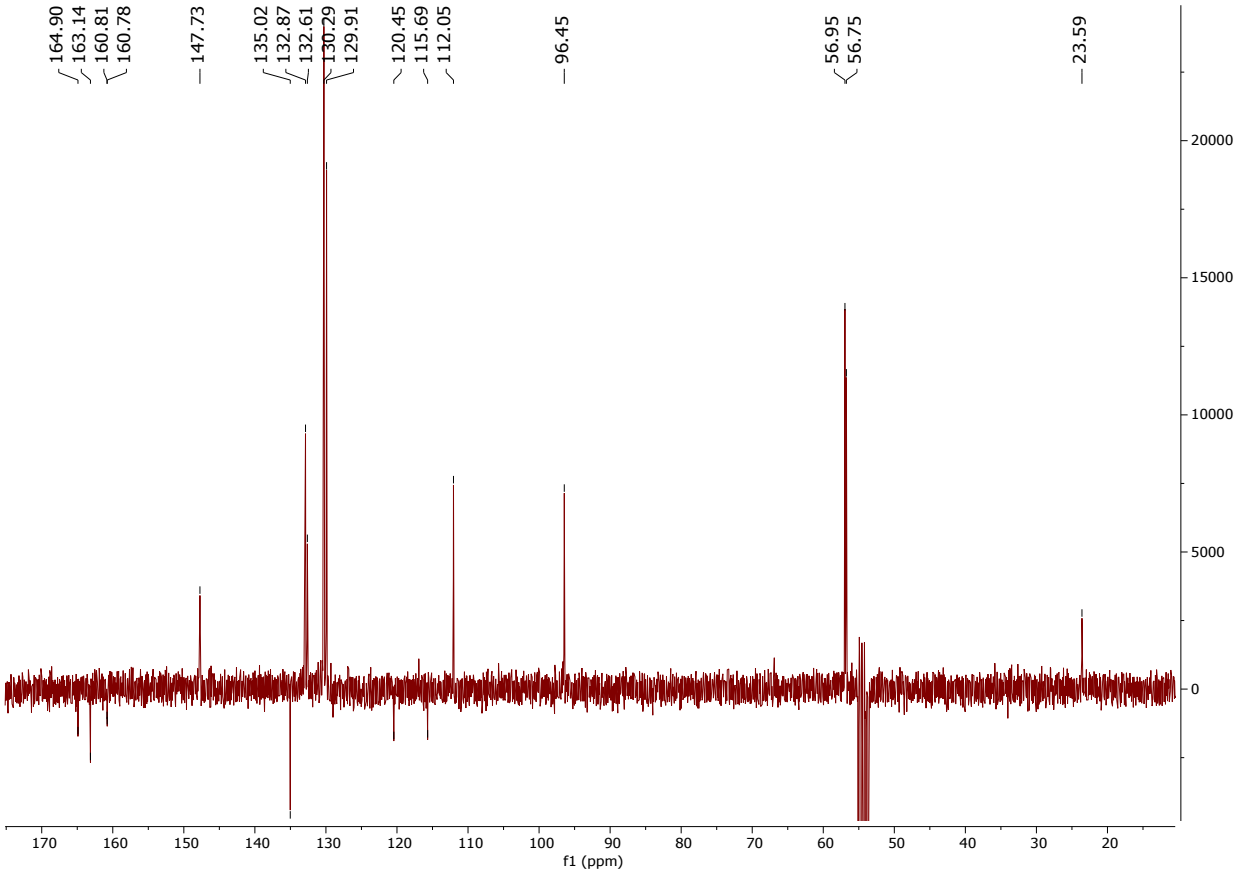

$^{13}C\{^{1}H\}$-(APT) NMR spectrum ($CDCl_3$, 75.47 MHz) of **4b**

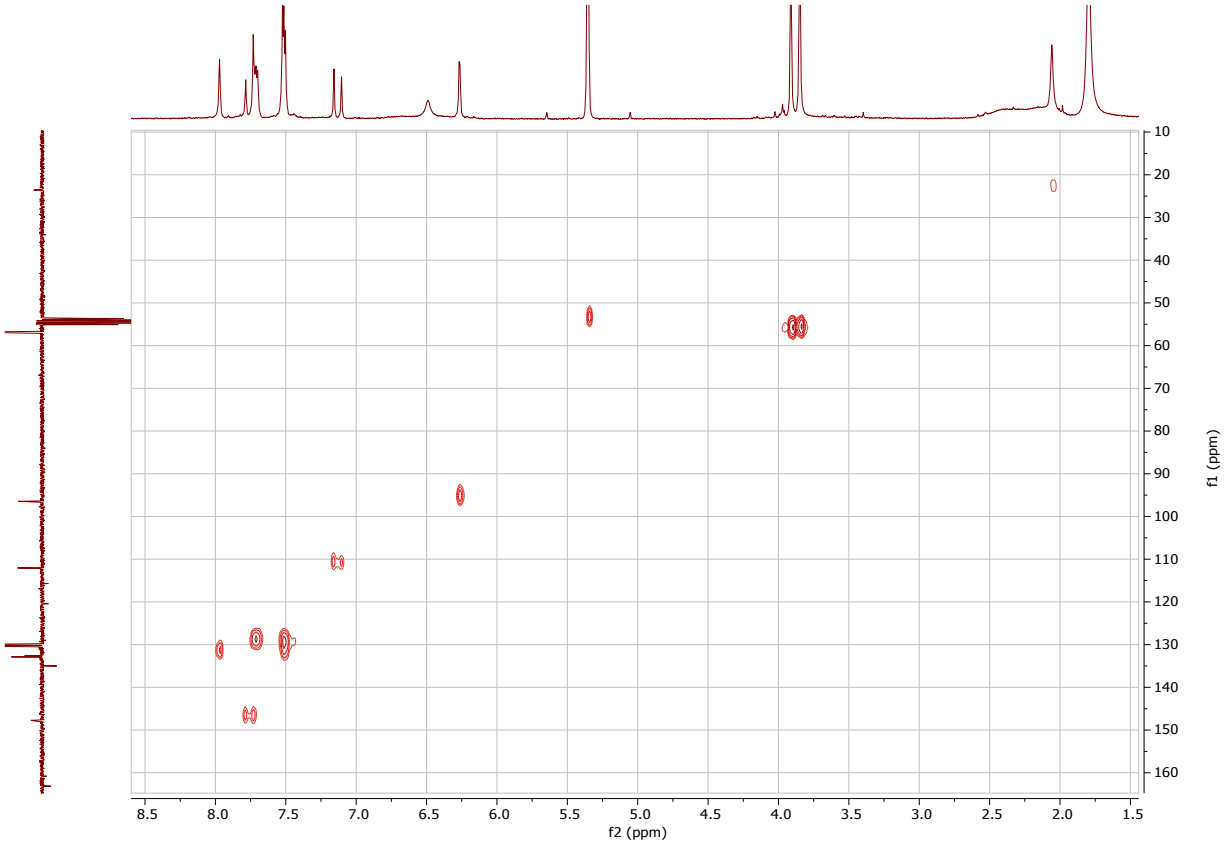

^{1}H-^{13}C HSQC correlation spectrum of **4b**

IR SPECTRA

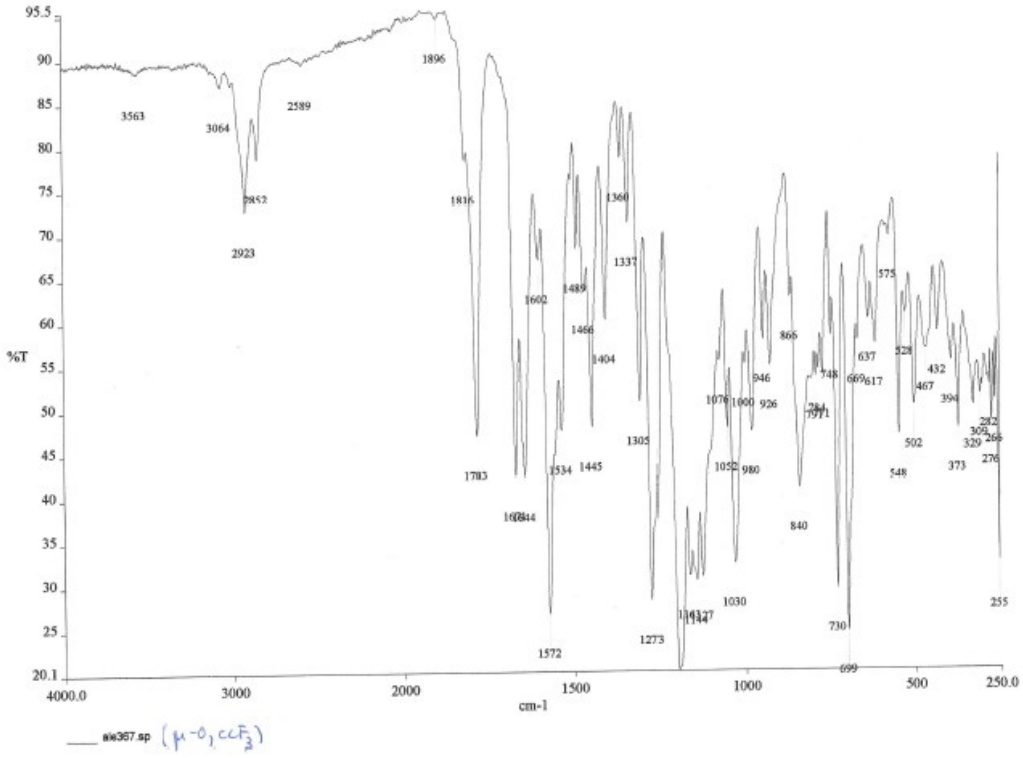

IR spectrum of **2ª**

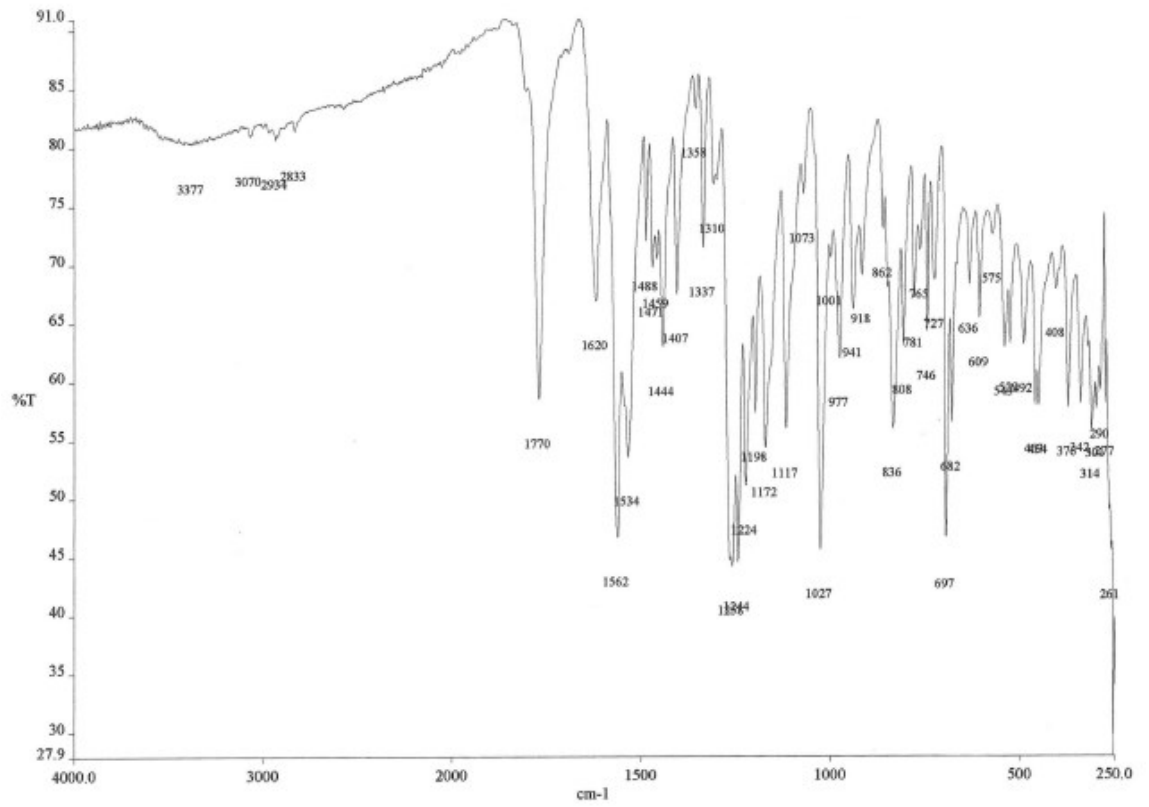

IR spectrum of **3ª**

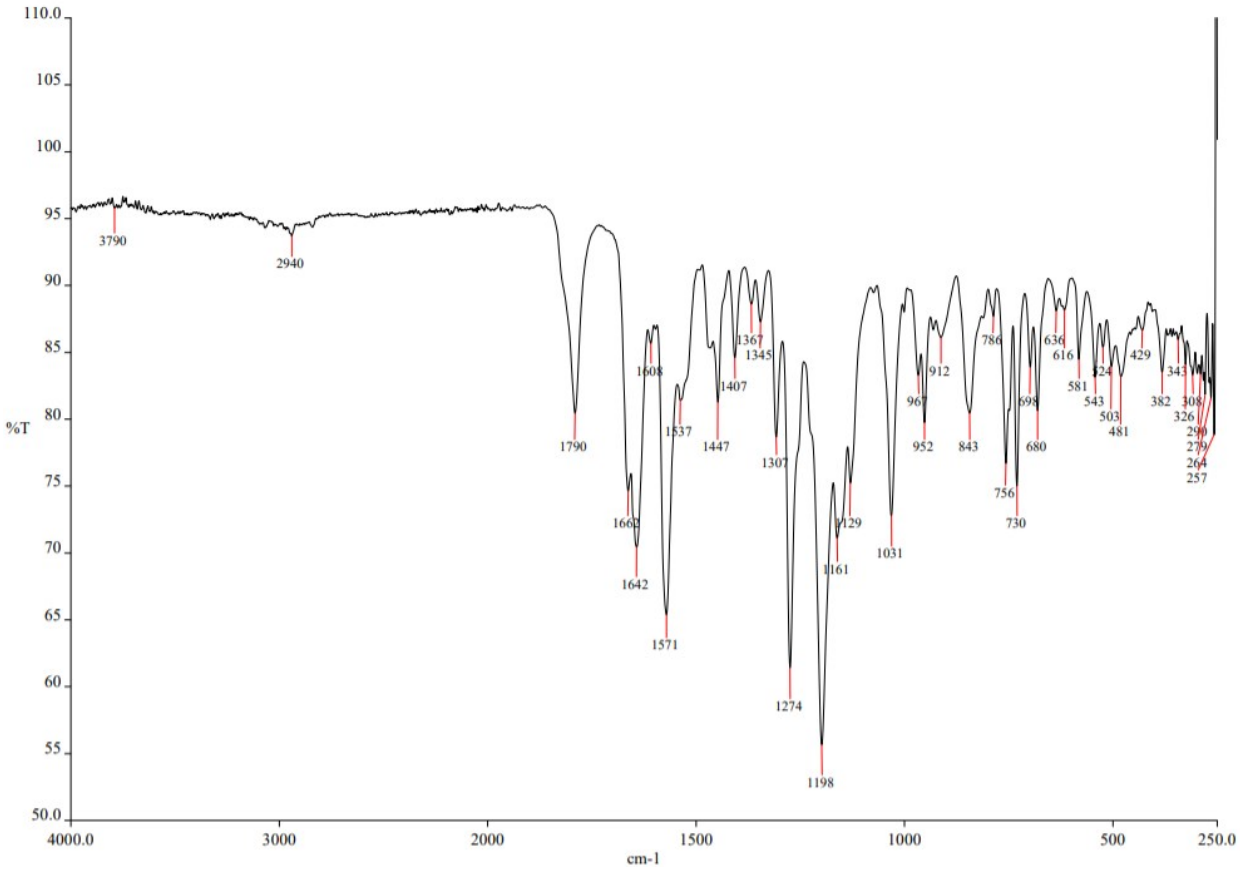

IR spectrum of **2b**

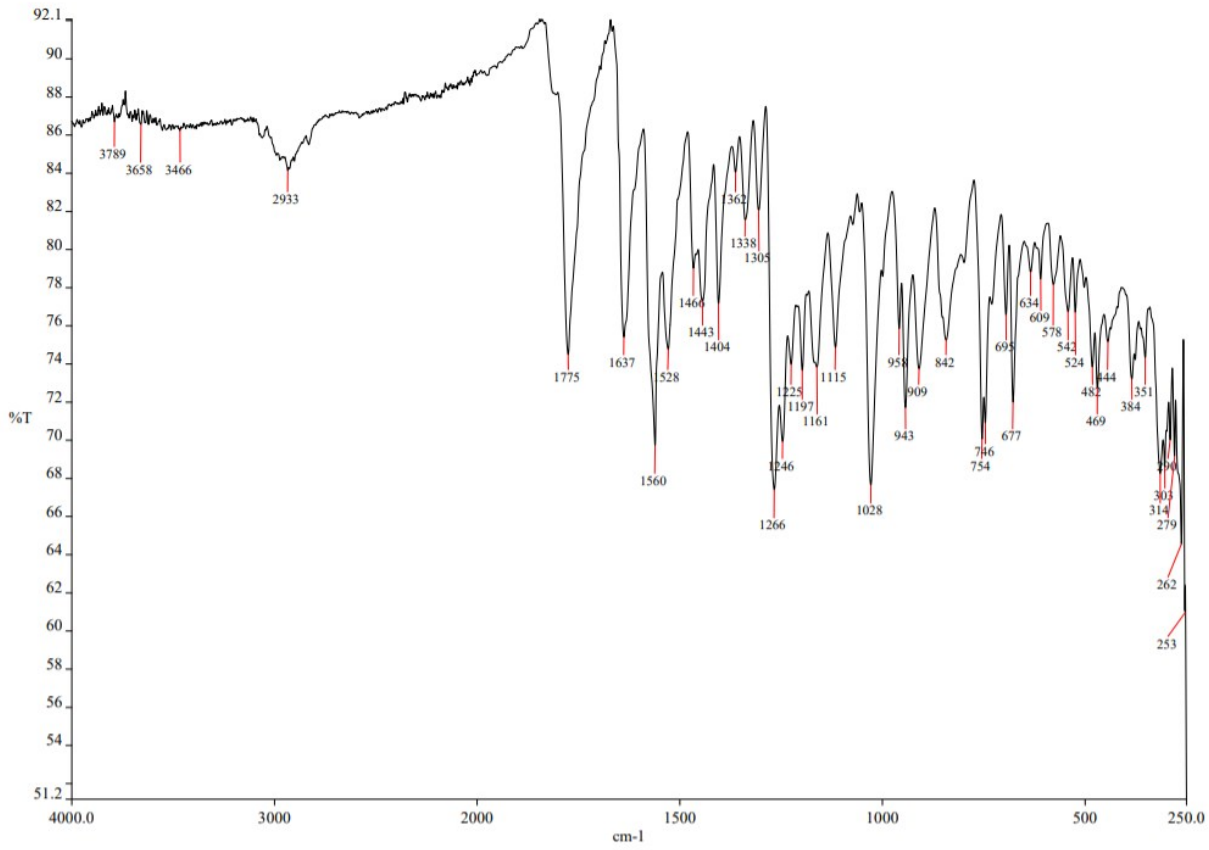

IR spectrum of **3b**